Ilmenite: A promising oxygen carrier for the scale-up of chemical looping

Pietro Bartocci [a,b,*], Alberto Abad [a,*], Arturo Cabello Flores [a], Margarita de las Obras Loscertales [a]

[a] CSIC, Instituto de Carboquimica, Zaragoza, Spain
[b] University of Perugia, Department of Engineering, Perugia, Italy

ABSTRACT

To tackle the scale-up of Chemical Looping Processes, the production of efficient and affordable oxygen carriers appears of paramount importance. Ilmenite is an ore-derived oxygen carrier which can be considered surely abundant and cheap. The preparation and the characterization of its reactivity are presented in the following paper. The paper describes briefly the performance of ilmenite relating it to other oxygen carriers, its thermodynamic properties, the kinetics and its use with fuels (solid, liquid and gaseous, including biofuels). Key features for an oxygen carrier are represented by costs and environmental sustainability, oxygen transport capacity and reactivity, as well as specific issues related to its use in fluidized bed reactors, namely agglomeration and attrition behavior. In addition, information about mutual interaction with fuel, considering also the influence of impurities, coke deposition or its effect on the gasification rate of solid fuels, is reported.

1. Introduction

Chemical looping processes promise to produce energy and/or hydrogen with CO_2 capture at low economic and energetic costs. According to Mendiara et al. [1], if we refer to biofuels, the chemical looping processes which can be performed are the shown in Fig. 1. These are mainly-three:

(a) chemical looping combustion (CLC) and chemical looping with oxygen uncoupling (CLOU);

(b) chemical looping reforming (CLR) or chemical looping gasification (CLG);

(c) chemical looping with water splitting (CLWS).

To these techniques we must add iG-CLC, defined as in-situ gasification chemical looping combustion. This process uses steam or carbon dioxide as gasification fluids adding them to the fuel reactor [2].

These processes evolved for 20 years from an incipient state of development up to reaching recently a level of maturity which can be identified as TRL6 for the combustion of solid fuels [1,3]. Further studies are required for the scale up of chemical looping processes to position it in a quasi-commercial status.

Oxygen carriers have a determining role on the features of Chemical Looping processes. The identification of a suitable material is crucial for the future scale-up of the chemical looping technologies and their development to achieve a commercially available chemical looping unit.

The use of ilmenite as an oxygen carrier was proposed by Leion et al. [4], who studied its main characteristics to be used in chemical looping combustion. Since then, a multitude of works have been done with ilmenite, focused on the production of heat by chemical looping combustion or hydrogen/syngas by chemical looping reforming/gasification processes. In addition, waiting for the development of chemical looping technologies, the use of ilmenite has been also proposed for the so-called oxygen carrier aided combustion (OCAC) in order to improve the combustion performance of fluidized bed boilers [5]. By means of these studies, the know-how on oxygen carrier materials, in this case ilmenite, to be used during long-term operating campaigns in Chemical Looping processes has been improved.

There are many reviews works analyzing oxygen carrier development for Chemical Looping Combustion and Reforming. Table 1 shows those that provide relevant information regarding the performance of ilmenite as oxygen carrier for chemical looping processes.

As we can see from the different reviews available in literature, it is still missing a complete review on ilmenite behavior in chemical looping combustion (CLC), chemical looping reforming (CLR), and oxygen carrier aided combustion (OCAC) processes. This review is based on the previous experience developed at the Instituto de Carboquimica in Zaragoza Spain.

Nomenclature

Abbreviations

AR	Air Reactor
ASU	Air Separation Unit
BET	Brunauer-Emmett-Teller Analysis
BFB	Bubbling Fluidized Bed
BFW	Boiler Feed Water
CAPEX	Capital Expenditure
CCS	Carbon Capture and Sequestration
CFB	Circulating Fluidized Bed
CFBC	Circulating Fluidized Bed Combustor
CFD	Computational Fluid Dynamics
CLC	Chemical Looping Combustion
CLG	Chemical Looping Gasification
CLOU	Chemical Looping with Oxygen Uncoupling
CLR	Chemical Looping Reforming
CLTR	Chemical Looping Tar Reforming
CLWS	Chemical Looping Water Splitting
CS	Carbon Stripper
DFT	Density Functional Theory
FR	Fuel Reactor
GtL	Gas-to-Liquids
GSC	Gas Switching Combustion
HHV	Higher Heating Value
iG-CLC	In-situ Gasification Chemical Looping Combustion
ITCMO	Iron-Titanium Composite Metal Oxide
LCOE	Levelized Cost of Electricity
LCOS	Levelized Cost of Steam
MSW	Municipal Solid Waste
NGCC	Natural Gas Combined Cycle
OC	Oxygen Carrier
OCAC	Oxygen Carrier Aided Combustion
OTSG	Once-Through Steam Generators
SAGD	Steam Assisted Gravity Drainage
SEM-EDX	Scanning Electron Microscopy-Energy Dispersive X-ray spectroscopy
TCR	Thermo-catalytic Reforming
TGA	Thermogravimetric analyzer
TRL	Technology Readiness Levels
XRD	X-ray diffraction
XRF	X-ray fluorescence

Greek letters

α	Fraction of elutriated oxygen carrier, which is recycled back (–)
ΔH_c^0	Standard heat of combustion of the gas fuel (kJ/mol)
ΔH_0^r	Heat of reaction (kJ/mol gas or C)
ΔP	Pressure drop (Pa)
ΔX_s	Solids conversion rate (–)
η_{CC}	CO_2 capture efficiency (–)
η_{CCS}	Efficiency of the CCS
ϕ	Oxygen carrier-to-fuel ratio (–)
ρ_m	Molar density of reacting material (mol/m^{-3})
τ_{chr}	Time for complete solids conversion when the chemical reaction controls the process (s)
τ_{dif}	Time for complete solids conversion when the diffusion controls the process (s)
ω_O	Mass based conversion (–)

Ω_T	Oxygen demand (–)

Symbols

b	Stoichiometric factor for the reaction (mol solid reactant per mol of fuel)
C_g	Gas concentration in the reactor (mol/m^{-3})
C_{g0}^n	Gas concentration at the reactor inlet (mol/m^{-3})
d	Stoichiometric factor in the fuel combustion reaction with oxygen (mol O_2 per mol of fuel)
D_e	Effective diffusivity in the product layer, (mol/m^{-2} s^{-1})
$D_{0,e}$	Pre-exponential factor for effective diffusivity in the product layer (mol/m^{-2} s^{-1})
E_a	Activation energy (kJ/mol)
E_{De}	Activation energy for the diffusion reaction (kJ/mol)
E_{ks}	Activation energy for the chemical reaction (kJ/mol)
F_{coal}	Rate of coal feeding (kg h^{-1})
F_{OC}	Solids circulation rate (kg h^{-1})
$f_{h,AR}$	Heat flow from the air reactor (% fuel power)
k_s	Chemical kinetic constant (mol^{1-n}m^{3n-2} s)
k_{s0}	Pre-exponential factor for chemical kinetic constant (mol^{1-n}m^{3n-2} s)
m	Instantaneous mass of oxygen carrier sample (g)
$\dot{m}_{loss}$	Oxygen carrier loss rate (–)
M_O	Molecular weight of oxygen (16 g mol^{-1})
$\dot{m}_{OC,min}$	Circulation rate of the oxygen carrier (kg oxygen carrier s^{-1} MW$_f^{-1}$)
m_{ox}	Mass of oxidised oxygen carrier (g)
m_{red}	Mass of reduced oxygen carrier (g)
P	Pressure (Pa)
$Q_{g,CS}$	Gas flow from carbon stripper (Nm^3 h^{-1})
$Q_{g,in}$	Inlet gas flow (Nm^3 h^{-1})
r_g	Grain radius (m)
R_g	Ideal gas constant (8.314 J mol^{-1} K^{-1})
r_o	Rate of oxygen transfer (s^{-1})
R_{OC}	Oxygen Ttansport capacity (–)
R_p	Particle radius (m)
t	Time (s)
T	Temperature (K)
T_{ex_FR}	Temperature at the exit of the fuel reactor (K)
T_{in_FR}	Temperature at the inlet of the fuel reactor (K)
u_{mf}	Minimum fluidization velocity (m/s)
u_{tf}	Throughflow gas velocity (m/s)
u_{vis}	Visible gas velocity of rising bubbles (m/s)
$V_{m,prod}$	Molar volume of reacting product (m^3/mol)
$V_{m,reac}$	Molar volume of reacting solid (m^3/mol)
W_{OC}	Cost of the oxygen carrier ($ kg^{-1})
x	Mass fraction (–)
X_{chr}	Solids conversion value from which reaction rate is controlled by diffusion (–)
X'_o	Modified solids conversion that takes into account that the diffusional control starts at the conversion X_{chr} (–)
$\overline{X}_{OC,in}$	Solid conversion at the fuel reactor inlet (–)
X_{ox}	Oxygen carrier conversion for the oxidation reaction (–)
X_{red}	Oxygen carrier conversion for the reduction reaction (–)
y_g	Gas volume fraction (–)
Z	Expansion ratio between the solid product and solid reactive (–)

2. Ilmenite chemical structure and main characteristics

Among iron-based oxygen carriers ilmenite has received much attention after the first tests carried out at Chalmers University [4,30–33]. It is a natural mineral containing iron oxide and titanium oxide with an indicative formula of $FeTiO_3$ [22]. The crystal structure of ilmenite is shown in Fig. 2. It can be compared with the structure of a spinel. The difference is that the spinel has a cubic structure while that of ilmenite is hexagonal. We can see from Fig. 2 that Fe^{2+} is tetrahedrally coordinated, while Ti^{4+} has an octahedral coordination, forming alternate layers inside an oxygen ions sub-lattice [34].

In reality it is very difficult to find the crystal structure presented in Fig. 2 in nature. In fact, in the alternate layers of ilmenite there is competition for the occupation of each site. In particular, the octahedral layer formed by titanium can be substituted by transition elements cations (Fe^{2+}, Cr^{3+}, Mn^{3+}), while divalent ions (Ca^{2+} and Mg^{2+}) can replace Fe^{2+}. As an example, Table 2 reports the composition of the ilmenite used by Symonds et al. [36], which has been provided by the company Rio Tinto Iron & Titanium, Québec, Canada. This composition has been determined by X-ray fluorescence (XRF) analysis following the ASTM D4326 method [37] on a completely oxidized sample.

The crystal of ilmenite can be seen alternatively also through XRD analysis. Fig. 3 shows the XRD patterns of a conventional ilmenite sample and of a pre-oxidized ilmenite. We can see that the only crystalline structure in raw ilmenite is represented by $FeTiO_3$. After oxidation three crystalline phases are formed: hematite (Fe_2O_3), pseudo-brookite (Fe_2TiO_5) and TiO_2.

As it is reported by Yu et al.[22], usually ilmenite can be completely oxidized by simply calcining it at a temperature comprised between 900 °C and 1200 °C in air atmosphere.

This is also a useful way to increase oxygen transport capacity, since as already seen, ilmenite contains mainly Fe^{2+}. After calcination the bivalent iron can be transformed in trivalent iron to form a Fe_2O_3/TiO_2 composite, see [39,40]. The calcination temperature affects deeply the behavior of ilmenite. If we consider a calcination process at 800 °C, it favors the formation of Fe_2O_3 and TiO_2. At higher temperatures, Fe_2TiO_5 and TiO_2 are formed [39,41]. An intermediate phase between ilmenite and pseudo-brookite can be considered as the following: $Fe_3Ti_3O_{10}$ ($Fe_3O_4 \cdot 3TiO_2$) [4].

In the study of Ridha et al. [42] it was also noted that calcination promotes the migration of iron to the surface of the particle, forming an iron-rich external shell (see Fig. 4). Cuadrat et al. [43] noted that the layer of iron increased its thickness with the increase of the number of redox cycles performed.

Iron migration is caused by the difference between the diffusivities of oxide ions and iron ions [44]. In the oxidation step, the outward diffusivity of Fe ions is higher than the inward diffusivity of O ions, then there is net Fe transport from the core of the Fe particle to the particle surface, where Fe_2O_3 is formed. This outward diffusion of Fe ions is further improved because the volume expansion of Fe particle during oxidation creates more physical space for Fe ion transport [19]. The application of density functional theory (DFT) calculations allows getting an insight into the ionic diffusion of oxygen carriers during chemical looping processes. In the particular case of ilmenite, Qin et al. [45] investigated the diffusion paths of Fe and Ti ions in oxygen carrier $FeTiO_3$ by combining first-principles micro-kinetics and ab initio thermodynamics. They found that the diffusion barrier of Fe ions was much lower than that of Ti ions. Therefore, the outward diffusion of Fe ions is more favorable than that of Ti ions leading to the segregation of both elements.

Some information is available in the literature about the theoretical capability of ilmenite to transfer lattice oxygen to gaseous fuels, e.g. CH_4, H_2 or CO. DFT calculations showed that oxygen diffusion in a Fe-Ti lattice is improved compared to pure Fe materials, e.g. hematite or magnetite, while steps related to the fuel adsorption of dissociation may be the rate determining ones [46]. Thus, H_2 molecule is strongly adsorbed on the Fe_2TiO_5 surface and the H—H bond is elongated [47]. Then, intermediates Fe-H and O—H bonds are formed, Fe-H bond is elongated and H approaches to an O—H form to eventually form H_2O. H atom diffusion from Fe-H bond has been determined to be the rate
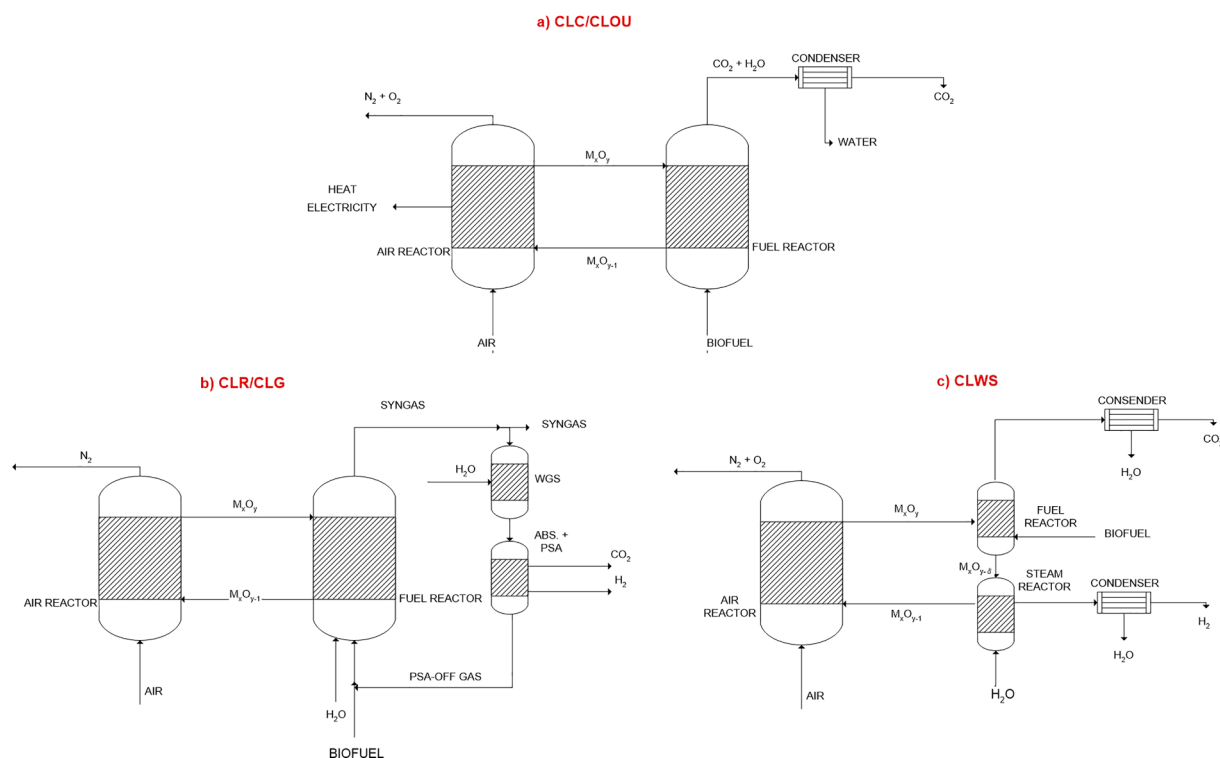

Fig. 1. Scheme of chemical looping processes with biofuels: (a) chemical looping combustion (CLC) and chemical looping with oxygen uncoupling (CLOU); (b) chemical looping reforming (CLR) or chemical looping gasification (CLG); and (c) chemical looping with water splitting (CLWS) [1].

Table 1
Reviews on chemical looping technologies that provide relevant information regarding the use of ilmenite as oxygen carrier.

Title	Source	Description
Use of ores and industrial products as oxygen carriers in chemical-looping combustion	Leion et al. 2009 [6]	This research work reported the good combustion performance of ilmenite for syngas, but not for CH_4. Ilmenite was tested in a laboratory fluidized bed setup using syngas and methane. Stability of the ilmenite after several cycles was detected. So, ilmenite met the criteria to be an appropriate OC, i.e., good reactivity, crushing strength and fluidization characteristics.
Oxygen carriers for chemical looping combustion-4 000 h of operational experience	Lyngfelt 2011 [7]	In this review, there is an overview table about experimental tests performed in different research centers and with different material including ilmenite. Testing time and fuel information are provided. The power plants ranged between 0.3 kW and 140 kW.
Progress in Chemical-Looping Combustion and Reforming technologies	Adánez et al. 2012, [8]	This is a comprehensive review of the Chemical-Looping Combustion (CLC) and Chemical-Looping Reforming (CLR) technologies up to 2010. This review gathers a very wide information about ilmenite in terms of agglomeration and reactivity. Ilmenite agglomeration occurred during oxidation after long reduction periods (from magnetite to wustite). No agglomeration issues were found during operation in a continuous unit. The addition of metal oxides to ilmenite may improve the combustion efficiency. Ilmenite undergoes an activation process after several redox cycles. An increase in porosity and reactivity of ilmenite particles occur with increasing the redox cycles, accompanied with an increase in its reactivity. The oxygen transport capacity decreases after 100 redox cycles. Ilmenite has high conversion of CO and H_2 for syngas applications, but moderate conversion of CH_4. A table with the kinetic determination of calcined and activated ilmenite is also included in this work.
Chemical looping processes—particle characterization, ionic diffusion–reaction mechanism and reactor engineering.	Zeng et al. 2012 [9]	Review focused on diffusion of atomic iron and oxygen through the ilmenite ($FeTiO_3$) structure. The effect of TiO_2 support can notably improve the ionic diffusivity of oxygen anion.
Fe–Mn based minerals with remarkable redox characteristics for chemical looping combustion	Larring et al. 2015 [10]	This research work makes a comparison between cheap iron and manganese based minerals with ilmenite. Tests were performed in a TGA. In addition to ilmenite, it is mentioned the existence of some minerals which are needless of pre-treatment prior to utilization in CLC, thus with great potentials due to omitting pre-treatment cost savings.
Chemical looping technology: oxygen carrier characteristics	Luo et al. 2015 [11]	This review deals with the development of oxygen carrier materials for chemical looping with full oxidation and with partial oxidation. The study of ilmenite for chemical looping with full oxidation is considered. The migration of iron to the surface of the ilmenite particle during oxidation is also commented. It is suggested that this phenomena could crack the ilmenite particle.
Chemical-Looping Combustion and Gasification of Coals and Oxygen Carrier Development: A Brief Review.	Wang et al. 2015 [12]	This review makes a comparison of reactivity among different iron bed materials including ilmenite. A comprehensive characterization of ilmenite after running test burning petcoke is discussed. Defluidization issues were detected at temperatures above 1000 °C. A table with the iG-CLC tests conducted with ilmenite in different plants and conditions is included. The high conversion of syngas (CO and H_2) and moderate conversion of CH_4 with ilmenite is mentioned. Likewise, this review reports that the coal rank has also an important role on the combustion efficiency because it depends on the conversion of the volatiles. It is suggested to better use steam than CO_2 as gasifying agent to prevent carbon fouling. Alkali addition is found to improve char gasification.
Present status and overview of Chemical Looping Combustion technology.	Nandy et al. 2016 [13]	This review compiles a table with different oxygen carriers that have been applied in continuous CLC units, including ilmenite. The table provides information about operational time and power plant for each case. Moreover, this review summarizes the main characteristics of ilmenite as oxygen carrier including reactivity with gases, particle lifetime of the material, activation phenomenon throughout redox cycles and sulfur resistance. Likewise, simulation and modelling works using ilmenite as oxygen carrier on CLC are briefly explained.
Oxygen carrier materials and their role in chemical looping reactions for fuel conversion.	Batra et al. 2017 [14]	In this paper, the recent trends in the development of oxygen carrier materials and their applications are discussed. In particular case of ilmenite, this paper describes the performance of this material in the largest CLC plant of $1MW_{th}$ using coal as fuel. Moreover, this review reports that the additions of metal oxides as NiO may improve the performance and the stability of the oxygen carrier.
CLC, a promising concept with challenging development issues.	Gauthier et al. 2017 [15]	This review provides the current price range of ilmenite and highlights that the mechanical stabilization and iron segregation may be an issue on long-term tests in continuous CFB pilot plants.
CO_2 capture with chemical looping combustion of gaseous fuels: an overview	Li et al. 2017 [16]	This review is focused on the technology of CLC with gaseous fuels. It gives a detail overview of the use of ilmenite as oxygen carrier for CLC process with gaseous fuels considering both atmospheric and pressurized systems.
Use of natural ores as oxygen carriers in chemical looping combustion: A review.	Matzen et al. 2017 [17]	This review collects works studying the use of natural ores in CLC including iron based, manganese-based, copper-based and calcium based ores. Regarding ilmenite, it is said that it shows a higher activity for H_2 conversion than for CO conversion. A table with the main results obtained using ilmenite for gaseous and solids fuels in CLC, including testing time and number of cycles, is also presented in this publication. Combination of other minerals with ilmenite leads to an increase in the conversion efficiencies of fuels. Likewise, the improvement of the reactivity of the ilmenite by adding alkali is commented. In this review, the activation of ilmenite with multiple redox cycles is explained because of the expansion of the pores in the ore.
Chemical looping combustion of solid fuels	Adánez et al. 2018 [18]	In this paper, the state of art of the CLC operation with solid fuels in existing facilities is reviewed an updated up to 2018. An overview of the most relevant results obtained in these units using ilmenite as oxygen carrier is presented. These results are evaluated based on the design and operating conditions used in each CLC unit as well as on the fuel selected.

(continued on next page)

Table 1 (*continued*)

Title	Source	Description
New insight into the development of oxygen carrier materials for chemical looping systems	Cheng et al. 2018 [19]	This review makes reference to the ionic diffusion mechanism of ilmenite. Naturally occurring ilmenite ($FeTiO_3$) shows an inward diffusion pattern for lattice oxygen in the bulk.
Chemical-looping technologies using circulating fluidized bed systems: Status of development.	Mattisson et al. 2018 [20]	This review describes the status development of CLC technologies using CFB reactors. Tables with information (power, oxygen carrier, fuel and testing time) related to chemical-operation with gaseous and solids fuels in CLC pilots can be found. Experience of the use of ilmenite for the Chemical Looping Tar Reforming (CLTR) process is also discussed.
Negative CO_2 emissions through the use of biofuels in chemical looping technology: A review.	Mendiara et al. 2018 [1]	This review gathers information about the use of ilmenite for syngas/H_2 production by means of reforming of tar components for upgrading of biomass-derived gas through CLR process. Moreover, the use of ilmenite for the combustion of biomass through the iG-CLC process is summarized. A table compiles the main experimental works carried out with biomass and ilmenite for the iG-CLC process. Experience of the use of ilmenite for the OCAC process is also considered.
Chemical-looping combustion: Status and research needs.	Adánez et al. 2019 [21]	This review summarizes the use of ilmenite in pilot testing for gaseous fuels. Moreover, the effect of the temperature on the CO_2 capture efficiency, combustion efficiency and oxygen demand in iG-CLC process for different solid fuels (coal and biomass) using ilmenite as oxygen carrier is analyzed.
Iron-based oxygen carriers in chemical looping conversions: A review.	Yu et al. 2019 [22]	This review is focused on the use of iron based oxygen carriers for chemical looping processes. A comprehensive summary of the physicochemical properties and main characteristics of ilmenite as oxygen carrier (crystalline phases, activation behavior, migration of iron) is performed. This review also states that the addition of alkali metals may enhance the reduction reactivity of ilmenite. Moreover, a table with information about continuous chemical looping operations with the iron-based oxygen carrier based on circulating fluidized bed systems (power, fuel, location) is also included.
11000 h of Chemical-looping combustion operation–where are we and where do we want to go	Lyngfelt et al. 2019 [23]	This paper discusses strategies for upscaling CLC technologies as well as the use of biomass for negative emissions. A table with detail information about the different CLC pilot plants and experiments performed with ilmenite and different fuels (coals and biomasses) is included. The power plants ranged between 0.3kW$_{th}$ and 1MW$_{th}$. Moreover, the use of ilmenite as bed material in a 75 MW$_{th}$ CFB for more than 12,000 h of operation obtaining satisfactory results in terms of combustion efficiency and performance is commented.
Development of stable oxygen carrier materials for chemical looping processes—A review	De Vos et al. 2020 [24]	This review aims to give more understanding of the selection and development of oxygen carrier materials for chemical looping Regarding ilmenite, it is said that the phase segregation phase (Fe-Ti) occurs after long-term operation. When pseudo-brookite (Fe_2TiO_5) is formed upon ilmenite oxidation, it segregates into Fe_2O_3 and TiO_2. The improvement of the CLC performance of ilmenite by adding CaO is also considered.
Chemical looping combustion: Status and development challenges.	Lyngfelt et al. 2020 [25]	This review collects relevant information about the status of CLC technology. A table related to the operational experience with ilmenite in CLC (1524 h) including pilot plants locations and fuels may be found herein. Likewise, the experience of 12000 h of oxygen carrier aided combustion (OCAC) mode with ilmenite is described.
Chemical-looping conversion of methane: a review.	Li et al. 2020 [26]	This review makes reference to the relatively slow reactivity of ilmenite with CH_4. As a consequence of that, the addition of metal oxides may improve its performance. The addition of metal oxides is contemplated not only to improve its reactivity towards CH_4. (ZrO_2, CeO_2, NiO, or Mn_2O_3) but also its oxygen transport capacity and reaction rate.
Developing Oxygen Carriers for Chemical Looping Biomass Processing: Challenges and Opportunities	Yu et al. 2020 [27]	This review is focused on the evaluation of oxygen carriers for Chemical Looping Biomass Processing. The high activity of ilmenite toward syngas conversion and tar reforming in the fuel reactor is highlighted. In addition, the high resistance against carbon deposition and Fe_3C formation, and segregation of iron to the surface of the particles are commented. A table providing information about crushing strength and surface area for different oxygen carriers including ilmenite can be also found herein.
Review of pressurized chemical looping processes for power generation and chemical production with integrated CO_2 capture.	Osman et al. 2021 [28]	This review summarizes the experimental techniques and operating conditions used for oxygen carrier reactivity and kinetics studies under high pressure, some of them carried out with ilmenite. The effect of total and partial pressure and temperature is analyzed.
Recent Advances and Development of Various Oxygen Carriers for the Chemical Looping Combustion Process: A Review	Qasim et al. 2021 [29]	This review discusses the criteria to select oxygen carriers: economic and environmental aspects, agglomeration, attrition, carbon deposition, oxygen vacancy, and oxygen transport capacity. Ilmenite ore is gaining interest due to its economic advantage. From tests in a fluidized bed, agglomeration issues with ilmenite at high temperatures, above 1050 °C are reported. TGA tests carried out with ilmenite showed that the attrition rate was increased with increasing number of cycles because of the increase in the surface porosity of the oxygen carrier.

determining step. It was also determined that the surface oxygen vacancy formation energy in Fe_2O_3 was decreased in the presence of Ti, which promotes the Fe_2TiO_5 reduction kinetics [48]. This fact may be of relevance when it is considered the mechanism of CH_4 conversion on Fe_2TiO_5, as it was concluded that oxygen migration ability is a key step in the CH_4 conversion to primary products, i.e. CO and H_2O [49]. Thus, the promotion of oxygen vacancies in Fe_2TiO_5 may facilitate the activation of adsorbed CH_4 by lowering its dissociation barriers [50].

Other important properties of ilmenite are the following: density, porosity and BET. These properties are reported in Table 3 and are taken from the work of Campos et al. [38]. The following instruments were used for characterization:
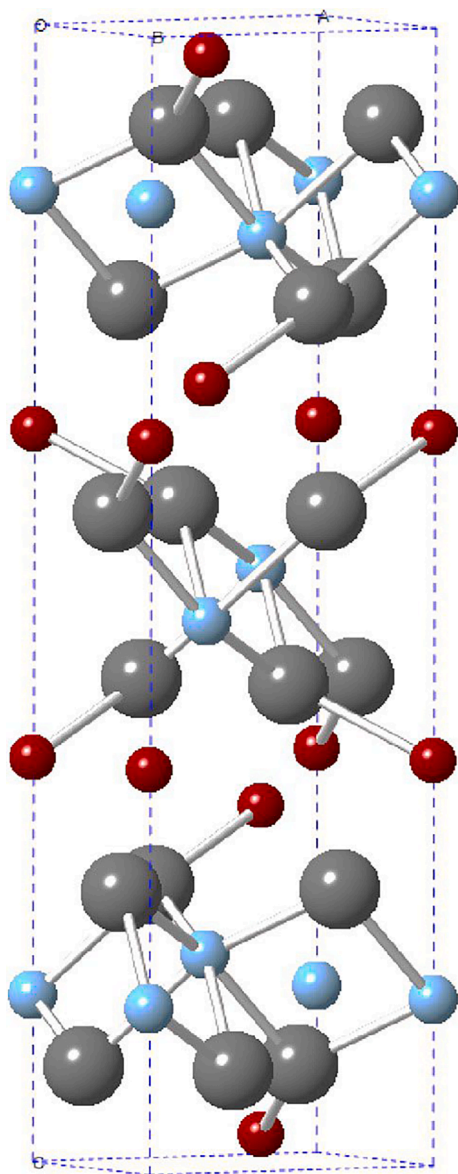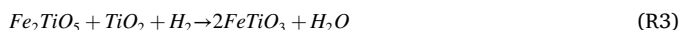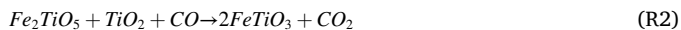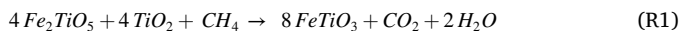
- An X-ray diffractometer Inel CPS 120 using an anticathode made of iron and filtered radiation of lambda equal to 1.936 $\dot{A}$. The ethane ionization curved detector allowed to read angles comprised between 2° and 120° (2θ = 5° −120°)
- The BET apparatus (Micromeritics ASAP 2020) operates in nitrogen atmosphere at −196 °C;
- Mastersize X laser diffraction analyzer for granulometric analysis;
- He pycnometry using an Accupyc 1330 from Micromeretics Instruments Inc.

The properties of the material were measured before and after 5 reduction cycles, performed in a SETARAM 92 TG-DT analyzer using
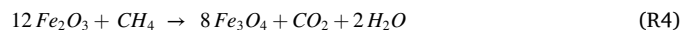
methane as reacting gas at 900 °C.

2.1. Ilmenite thermodynamic behavior

As above mentioned, ilmenite is mainly composed of iron titanium oxide $FeTiO_3$, i.e. the reduced form of the oxygen carrier. Its oxidized form is pseudo-brookite (Fe_2TiO_5), being this the solid with the capability to transfer oxygen. However, commonly the oxygen carrier is named as ilmenite. Main reacting gases in chemical looping processes are CH_4, CO and H_2. Reactions (1–3) show the processes corresponding to the reduction of pseudo-brookite to ilmenite:

$$4\,Fe_2TiO_5 + 4\,TiO_2 + CH_4 \rightarrow 8\,FeTiO_3 + CO_2 + 2\,H_2O \qquad (R1)$$

$$Fe_2TiO_5 + TiO_2 + CO \rightarrow 2FeTiO_3 + CO_2 \qquad (R2)$$

$$Fe_2TiO_5 + TiO_2 + H_2 \rightarrow 2FeTiO_3 + H_2O \qquad (R3)$$

Fig. 2. Crystal structure of ilmenite mineral (O = grey, Ti = blue, Fe = red) [35]. (For interpretation of the references to colour in this figure legend, the reader is referred to the web version of this article.)

The presence of hematite (Fe_2O_3) in the ilmenite particles was also found to be part of the original composition of the mineral. In this regard, many XRD analyses of fresh samples of ilmenite used as oxygen carriers in CLC processes have detected the presence of Fe_2O_3 as one of the main compounds of this ore. The reduction of hematite in chemical looping processes is described by reactions (4–6).

$$12\,Fe_2O_3 + CH_4 \rightarrow 8\,Fe_3O_4 + CO_2 + 2\,H_2O \qquad (R4)$$

$$3Fe_2O_3 + CO \rightarrow 2Fe_3O_4 + CO_2 \qquad (R5)$$

$$3Fe_2O_3 + H_2 \rightarrow 2Fe_3O_4 + H_2O \qquad (R6)$$

Further reduction of $FeTiO_3$ to $Fe + TiO_2$ or Fe_3O_4 to FeO/Fe is not of interest for chemical looping combustion, as it entails a high amount of unconverted H_2 and CO at equilibrium conditions. In addition, reduction to $FeTiO_3$ and Fe_3O_4 has been also found, when a partial oxidation of the fuel is desired, e.g. to obtain syngas, i.e. a gas mixture mainly composed by H_2 and CO. For example, this was the case of chemical looping gasification of biomass [51].

The Gibbs energy variation of ilmenite reduction is shown in Fig. 5.

As it can be seen from Fig. 5, the reduction reactions start to happen in a temperature interval comprised between 500 °C and 900 °C, in correspondence of negative values of the Gibbs free energy. Carbon monoxide is the reducing agent which requires less temperature to start the reaction. Reduction with methane starts happening at a temperature equal to 600 °C. Reduction with hydrogen starts happening at temperatures equal to 900 °C. The heat of oxidation and reduction reactions involving ilmenite is reported in Table 4, data are taken from [8].

Therefore, the oxidation reactions involved in the air reactor when ilmenite is used as oxygen carrier, are described by reactions (7–8).

$$4FeTiO_3 + O_2 \rightarrow 2Fe_2TiO_5 + 2TiO_2 \qquad (R7)$$

$$4Fe_3O_4 + O_2 \rightarrow 6Fe_2O_3 \qquad (R8)$$

The mass variation between the oxidized and reduced states corresponds to the transfer of oxygen from the solid to the fuel [40]. Thus, the oxygen transport capacity of the material, R_{OC}, is defined as follows:

$$R_{OC} = \frac{m_{ox} - m_{red}}{m_{ox}} \qquad (E1)$$

where m_{ox} and m_{red} are the masses of the oxidized ($Fe_2TiO_5 + Fe_2O_3$) and reduced ($FeTiO_3 + Fe_3O_4$) forms of the oxygen carrier, respectively, as it was indicated by reactions (R1)-(R8).

As the oxygen transport capacity for the redox pair Fe_2O_3/Fe_3O_4 ($R_{OC,Fe2O3} = 3.3$ wt%) is lower than that for the redox pair $Fe_2TiO_5/FeTiO_3$ ($R_{OC,Fe2TiO5} = 5.0$ wt%), it is expected that the oxygen transport capacity decreases with the redox cycles when Fe_2O_3 fraction increases at the expense of Fe_2TiO_5 after the activation process takes place. Thus, the oxygen transport capacity of ilmenite is calculated as a function of the mass fraction of Fe_2TiO_5, $x_{Fe2TiO5}$, and Fe_2O_3, x_{Fe2O3}:

$$R_{OC} = R_{OC,Fe_2TiO_5} x_{Fe_2TiO_5} + R_{OC,Fe_2O_3} x_{Fe_2O_3} \qquad (E2)$$

Another interesting characteristic of ilmenite is that it can release small amounts of oxygen directly when heated at temperatures higher than 950 °C [53]. The oxygen released accounts for 0.1v% of the total oxygen concentration in the gas which passes through the chemical looping fluidised bed reactors. The process is probably due to the presence of a small quantity of manganese in the ilmenite or to the interaction of Mn with Fe or Ti.

2.2. Mass and enthalpy balances

The analysis of the influence of the thermochemical properties of ilmenite on its performance as an oxygen carrier has been mainly focused on chemical looping combustion. The enthalpies of the involved reactions together with the oxygen transport capacity, R_{OC}, are two

Table 2
Composition of an ilmenite sample [37].

Component	Quantity	Unit of measure
SiO_2	< 0.10	wt%
Al_2O_3	0.36	wt%
Fe_2O_3	60.90	wt%
TiO_2	36.50	wt%
P_2O_5	< 0.03	wt%
CaO	< 0.05	wt%
MgO	1.72	wt%
SO_3	< 0.10	wt%
Na_2O	< 0.20	wt%
K_2O	< 0.02	wt%
Barium	1927	ppm
Strontium	< 50	ppm
Vanadium	1350	ppm
Nickel	302	ppm
Manganese	985	ppm
Chromium	752	ppm
Copper	164	ppm
Zinc	71	ppm
Loss of fusion	0.00	ppm

fundamental aspects to determine one of the main design parameters of a CLC process, i.e., the solids circulation rate.

The required solids circulation rate to supply oxygen from air to fuel depends on the oxygen carrier and the fuel used, and is calculated by:

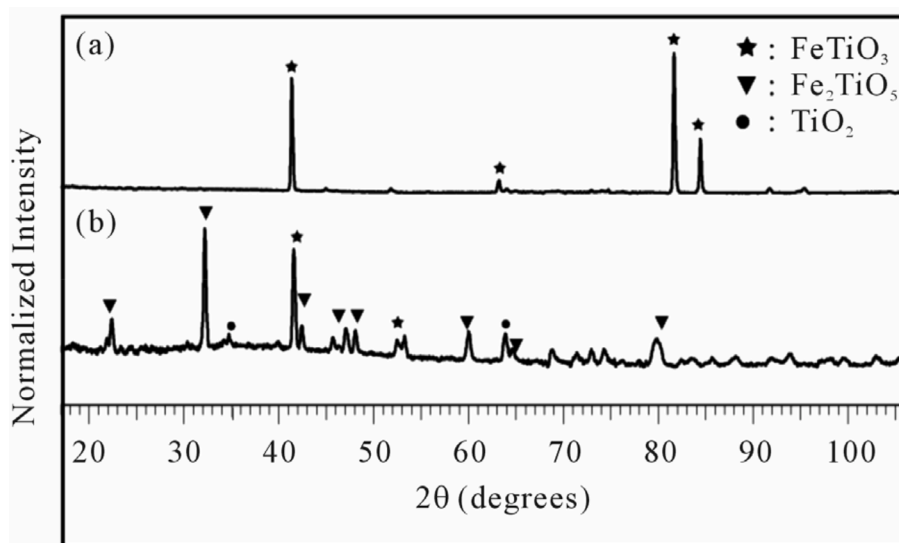$$\dot{m}_{OC,min} = \frac{2 \bullet d \bullet M_o}{R_{OC} \Delta H_c^0} \tag{E3}$$

The $\dot{m}_{OC,min}$ parameter is the minimum solids circulation rate required in a CLC system, which implies that all the available oxygen in the oxygen carrier is transferred, i.e. the oxygen carrier is completely oxidized in the air reactor and fully reduced in the fuel reactor. Higher solids circulation rates may be suitable in order to decrease the variation of the solids conversion, ΔX_s, and it can be expressed as follows:

$$\dot{m}_{OC} = \frac{\dot{m}_{OC}}{\Delta X_s} = \frac{2 \bullet d \bullet M_o}{R_{OC} \Delta H_c^0} \bullet \frac{1}{\Delta X_s} \tag{E4}$$

where d is the stoichiometric factor in the fuel combustion reaction with oxygen, M_o is the molecular weight of oxygen, R_{OC} is the oxygen transport capacity of the oxygen carrier, ΔH_c^0 is the standard heat of combustion of the gaseous fuel, and ΔX_s is the variation of solids conversion. Fig. 6 shows the solids circulation rate for the particular case of

Table 3
Characterization of raw and reacted ilmenite [38].

Analysis	Pre-oxidized ilmenite	Reacted ilmenite (5 reduction cycles)
XRD (main species)	Fe_2TiO_5, TiO_2, $FeTiO_3$	T < 800 °C: $FeTiO_3$, TiO_2, Fe_3O_4 T greater than 800 °C: Fe_2TiO_5, TiO_2, $FeTiO_3$
True density	4575 kg m^{-3}	4110 kg m^{-3}
Porosity	16.07 %	36.72 %
Particle diameter	25–300 µm	25–300 µm
BET Surface	0.10 m^2/g	0.21 m^2/g

Fig. 3. Crystalline structure of a) raw ilmenite and b) pre-oxidized ilmenite [38].
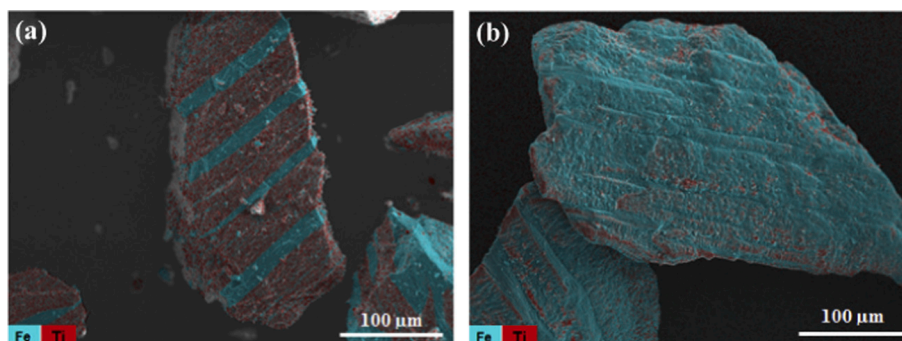
Fig. 4. Migration of iron to the surface after calcination of ilmenite: a) raw, b) calcined [42].

ilmenite, expressed as kg of oxygen carrier per second and MW of fuel, as a function of the variation of the solids conversion for three different fuels, i.e., CH$_4$, CO and H$_2$.

Taking as reference a value of 16 kg s^{-1} MW^{-1} as the maximum solids circulation rate in circulating fluidized bed commercial units [54], the minimum variation of solids conversion required in CLC plants that use ilmenite as oxygen carrier for the combustion of CH$_4$, CO and H$_2$ is 0.13, 0.09, and 0.10, respectively. Moreover, in general, ΔX_s values close to 1 would not be advisable either, since it would imply a very important increase in the solids inventory necessary in the fuel and air reactors to completely reduce or oxidize the oxygen carrier particles in each redox semi-cycle. The optimum values of ΔX_s to achieve low solids circulation rates and low solids inventories are between 0.2 and 0.4 [54]. These values could be suitable if ilmenite were used as oxygen carrier.

In a CLC process, the oxidation reaction happening in the air reactor between the reduced oxygen carrier and the oxygen present in the air stream is always exothermic. The reduction reaction between the oxidized oxygen carrier and the fuel fed to the fuel reactor can be exothermic or endothermic, depending on the redox system considered. However, the addition of the enthalpy variation in the fuel and air reactors is the same as that of a conventional combustion process, in which fuel and air are in direct contact. In a common configuration, with 20 % or less of excess air, the enthalpy transferred to the gases exiting the CLC unit –namely, combustion gases and exhaust air– is lower than the combustion enthalpy. This fact entails that a significant release of heat must be removed from the solids and recovered through a heat recovery system to fulfil the energy balance of the CLC unit. The heat recovery system may be avoided by working at high air excess ratios, thus having extra enthalpy present in the exhaust air stream. However, this option implies a high energy demand for the blower which feds a high air flow to the air reactor.

In the particular case of ilmenite, the reduction with CH$_4$ is endothermic, whereas the reduction with CO is exothermic. With H$_2$, the reduction reaction is slightly exothermic at room temperature ($\Delta H_r^0 = $ -14.6 kJ/mol H$_2$) [8], but at the typical operating temperatures in a CLC process, i.e., 800 °C-1000 °C, the reaction becomes slightly endothermic. Regarding the oxidation reaction, the standard heat of reaction, ΔH_r^0, for the redox pair Fe$_2$TiO$_5$/FeTiO$_3$ is -454.5 kJ/mol O$_2$ [8]. In this regard, Hallberg et al. [55] experimentally determined the enthalpy for the oxidation reaction of three different ilmenite particles at a temperature of 950 °C. Theoretically, at this temperature, the enthalpy for the oxidation reaction (R7) is 445 kJ/molO$_2$. In that work, the obtained values were slightly higher, between 453 and 469 kJ/mol O$_2$. One possible explanation was that reaction R(7) was not the only oxidation

reaction that took place. The authors explain that the presence of Fe$_2$O$_3$ in ilmenite particles may modify the enthalpy balance in the system. Thus, part of the oxygen transferred in the particles was between the redox pair Fe$_2$O$_3$/Fe$_3$O$_4$; this explains why the enthalpy corresponding to the oxidation semi-cycle (reaction R(8)) has a higher value of 480 kJ/mol O$_2$.

Experimentally, it has been found that Fe and Ti atoms have a tendency to migrate inside the ilmenite particles to form hematite, Fe$_2$O$_3$, and rutile, TiO$_2$ [40,42,43,56]. This accumulation of Fe$_2$O$_3$ in the particles might cause that the enthalpy balance in the fuel and air reactors varies with the length of the time period during which the ilmenite particles have been used.

As above mentioned, in a CLC system the mass balance is closely related to the enthalpy balance. In fact, the solids circulation rate between the reactors has a great influence on the mass and enthalpy balances in a CLC unit, since this parameter has to be high enough to transfer the oxygen necessary for the fuel combustion and the heat necessary to maintain the temperature in the fuel reactor when the reduction reaction is endothermic [54].

Fig. 6 also shows that the temperature difference in the fuel reactor between the incoming and exiting solids depends on the fuel used by means of the heat of reaction and the variation of solids conversion, ΔX_s, which depends indeed on the solids circulation rate. In this case, it is assumed that the fuel reactor is adiabatic, the temperature at the outlet of the air reactor is 1000 °C, and the air excess is 20 % over the stoichiometric amount necessary to completely convert the fuel. The temperature difference is higher when the solids recirculation rate is lower. For the endothermic reaction of CH$_4$ with ilmenite, a drop in temperature occurs in the fuel reactor. This drop can reach up to almost 100 °C if ilmenite particles are completely reduced; so very low solids circulation rates are not recommended in order to avoid significant temperature variations between the reactors. In the case of CO, the situation is the opposite, since the reaction with ilmenite is exothermic and there is an increase in the temperature in the fuel reactor. Besides, there is a minimal drop of temperature in the fuel reactor when H$_2$ reacts with ilmenite, because the reaction is slightly endothermic at these temperatures. Finally, Fig. 6 shows the effect of the variation of the solids conversion in ilmenite particles on the percentage of thermal power that can be removed from the solids in the air reactor, $f_{h,AR}$. This parameter takes a value between 50 and 60 % for all the selected fuels, regardless of the ΔX_s value.

2.3. Redox behavior of ilmenite: reactivity and kinetics

As indicated by Abad et al. [57] there are two important reactor design parameters which are deeply correlated with kinetics: reactor inventory and oxygen carrier circulation rate. These two parameters are also interconnected to each other and depend on the reactivity of the materials and their oxygen transport capacity [54]. The oxygen carrier needs to have enough reactivity to be reduced by the fuel and oxidized by air in the air reactor. To design properly a CLC reactor it is needed to
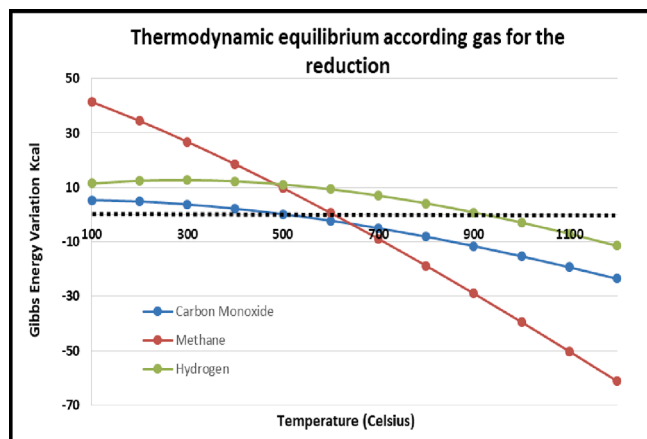
Fig. 5. Thermodynamic analysis performed with the software HSC 5 Chemistry Version 6.0 to evaluate Gibbs free energy of the reduction reactions performed with different reducing agents (carbon monoxide, methane and hydrogen) [52].

Table 4
Standard heat of reaction (ΔH_0^r) for the reduction and oxidation with ilmenite and hematite [8].

Reaction	Value	Unit of measure
CH$_4$ + Fe$_2$TiO$_5$/FeTiO$_3$	106.5	kJ/mol gas or C
H$_2$ + Fe$_2$TiO$_5$/FeTiO$_3$	-14.6	kJ/mol gas or C
CO + Fe$_2$TiO$_5$/FeTiO$_3$	-55.8	kJ/mol gas or C
C + Fe$_2$TiO$_5$/FeTiO$_3$	60.9	kJ/mol gas or C
O$_2$ + Fe$_2$TiO$_5$/FeTiO$_3$	-454.4	kJ/mol gas or C
CH$_4$ + Fe$_2$O$_3$/Fe$_3$O$_4$	141.6	kJ/mol gas or C
H$_2$ + Fe$_2$O$_3$/Fe$_3$O$_4$	-5.8	kJ/mol gas or C
CO + Fe$_2$O$_3$/Fe$_3$O$_4$	-47.0	kJ/mol gas or C
C + Fe$_2$O$_3$/Fe$_3$O$_4$	78.4	kJ/mol gas or C
O$_2$ + Fe$_2$O$_3$/Fe$_3$O$_4$	-472.0	kJ/mol gas or C

investigate the behavior of the oxygen carrier under different reaction conditions. Also, to predict satisfactorily the experimental results of the pilot plant with the mathematical model, it is necessary to know the real reactivity of ilmenite particles and determine the kinetic parameters for the described reactions (R1-R8).

It is well known that ilmenite particles increase their reactivity with the redox cycles [40]. This process has been referred to as an activation process, which depends on the reacting conditions existing in every reduction and oxidation semi-cycle. Typically, the oxygen carrier is partially reduced during its operation in a CLC unit, while it is highly oxidized in the air reactor [58]. In contrast, the reaction progress under CLG conditions has been found to be different: the oxygen carrier is highly reduced in the fuel reactor, while it is partially oxidized in the air reactor [51].

Ilmenite has been extensively evaluated as an oxygen carrier for the combustion of gaseous and solid fuels in several facilities, including TGA, batch fluidized bed reactors and continuous CLC units. Recently, this material has been also tested for the CLG process at 1.5 kW scale [51]. In these processes, ilmenite is cyclically reduced and oxidized, according to the reactions (R1)-(R8). The chemical stress, triggered during consecutive redox cycles, affects the physicochemical properties of the ilmenite particles. Table 5 reports information about the effect of redox cycles on the evolution of different properties of ilmenite particles.

Ilmenite, as received, has not porosity, and it is mainly composed by $FeTiO_3$ and Fe_2O_3. After the pre-oxidation period, ilmenite is fully oxidized to Fe_2TiO_5, while some Fe_2O_3 remains in the solid. During this process, ilmenite particles gain some porosity (1.2 %). However, the reactivity with reducing gases (CO, H_2 and CH_4), as well as for oxidation

with O_2, is quite low; see *Rate Index* values in Table 5. The reactivity of oxygen carriers is often evaluated by using the *Rate Index* parameter, which is defined as follows: [59].

$$Rate\ Index\ (\%/\min) = 100 \cdot 60 \cdot \frac{y_{g,ref}}{y_g} \left| \frac{d\omega_0}{dt} \right| \qquad (E5)$$

The mass based conversion, ω_O, and the rate of oxygen transfer, r_O, may be calculated as follow:

$$\omega_O = \frac{m}{m_{ox}} = 1 - R_{oc} \bullet X_{red} = 1 - R_{oc}(1 - X_{ox}) \qquad (E6)$$

$$r_O = \left| \frac{d\omega_O}{dt} \right| = R_{OC} \left| \frac{dX_i}{dt} \right| \qquad (E7)$$

The reduction conversion reached in each cycle has an important effect on the physic-chemical changes observed in ilmenite.

SEM pictures of pre-oxidized and activated particles can be seen in Fig. 7. For pre-oxidized ilmenite a granular structure of the solid is observed, which is enhanced by repeated redox cycles, together with again in porosity. The porosity of calcined ilmenite was 1.2 %, whereas for reacted ilmenite the porosity value was as high as 35 % after 100 redox cycles. From SEM observation, the mean size of the grains was determined to be about 1 μm for calcined ilmenite and about 2.5 μm for activated ilmenite. Fig. 8(a) compiles the available porosity data from tests showed in Table 5. The chemical stress induces an increase in the porosity. Thus, the increase in the porosity is promoted by the increase in the variation of the solids conversion, ΔX_s.

In addition to porosity, the crushing strength was affected by the chemical stress; see Fig. 8(b). Crushing strength measures were made for fully oxidized as well as fully reduced samples, and both samples had a similar value for crushing strength. Pre-oxidized ilmenite particles had relatively high values of crushing strength, namely 2.2 N. This value for the crushing strength would be acceptable for the use of these particles in circulating fluidized-beds [63]. Crushing strength increased during the first 20 redox cycles to around 2.9. However, particles after 50 and 100 cycles showed a decrease in crushing strength, which was below a value of 1 N after 100 cycles. 1 N is considered the generally accepted threshold value in order to prevent abrasion and breakage issues typical in fluidized beds.

Table 5 shows the chemical composition obtained by XRD analysis for pre-oxidized and reacted ilmenite under several operating conditions and facilities: TGA, batch fluidized-bed reactor and CLC unit. Pre-oxidized and reacted particles revealed ferric pseudo-brookite (Fe_2TiO_5), rutile (TiO_2) and some free hematite (Fe_2O_3) as major components. Besides, SEM-EDX analyses revealed a Fe:Ti molar ratio around 1:1. In the fully oxidized ilmenite, the iron was found to be as Fe^{3+}, either in the Fe_2TiO_5 compound or as free Fe_2O_3. During reaction with CO, H_2 or CH_4, Fe^{3+} in these compounds is reduced to $FeTiO_3$ and Fe_3O_4, respectively, regardless CLC or CLG conditions are considered. During redox reactions, the solid structure changes from trigonal $FeTiO_3$ to orthorhombic Fe_2TiO_5, and TiO_2 must move in and out from the Fe-Ti crystalline structure; see reactions (R1)-(R8). These changes induce a relevant chemical stress, but reaction also promotes the migration of iron to the particle surface, being detached form the titanium rich nucleus in the particle; see Fig. 9. It was observed that there is a gradual migration of iron forming an external shell, which grows with the redox cycles both under CLC and CLG conditions.

Migration of iron modifies the chemical composition of the ilmenite particles. Fig. 10(a) shows the mass fraction of Fe_2TiO_5 and Fe_2O_3 in the ilmenite particles as a function of the number of cycles for different variations of the solids conversion, namely $\Delta X_s = 0.2$ and 0.55. As the number of cycles increases, the fraction of free Fe_2O_3 rises at the expense of Fe_2TiO_5 when $\Delta X_s = 0.55$. However, the composition was roughly constant at the lower value of $\Delta X_s = 0.2$. This fact suggests that the migration of iron is also promoted by the chemical stress, i.e. there is a higher degree of iron migration as ΔX_s increases, being of low relevance
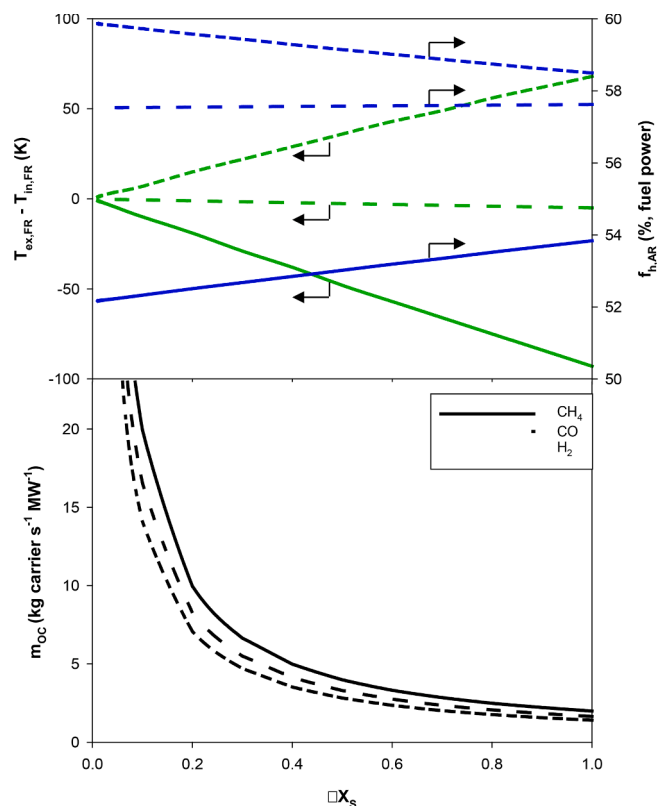

Fig. 6. Relation between the variation of solids conversion (ΔX_s) and the solids circulation rate, $\dot{m}_{OC}$, the temperature difference in the fuel reactor between the incoming and exiting solids, and the fractional heat flow extracted from the solids respect to the total input fuel power, $f_{h,AR}$. The temperature at the outlet of the air reactor is 1000 °C, the fuel reactor is adiabatic, air ratio = 1.2, and the inlet temperature of the fuel and air streams is 25 °C.

when ΔX_s is low.

The composition of ilmenite has relevance on the amount of oxygen that the solid particles can transfer from the air reactor to the fuel reactor, i.e. the oxygen transport capacity of ilmenite, R_{OC}, as it was shown in equation (E.2). The calculated values for the oxygen transport capacity of pre-oxidized ilmenite is $R_{OC} = 4.0$ wt%. Fig. 10(b) shows that the oxygen transport capacity decreases when reacting conditions promoted the iron migration and segregation, e.g. $\Delta X_s = 0.55$. However, the oxygen transport capacity barely decreased when ΔX_s values were as low as 0.2, condition under which migration and segregation of iron were of lower relevance. The theoretical R_{OC} value calculated from equation (E.1) was confirmed by TGA tests with suitable reacting conditions, namely, using a flow composed of 5 vol% H_2 and 40 vol%H_2O, in order to limit the reduction of Fe_2TiO_5 and Fe_2O_3 to $FeTiO_3$ and Fe_3O_4, respectively [43].

The chemical stress also modified the reaction rate of the oxygen carrier. Because the reactivity is characterized by dX_i/dt, Fig. 11(a) shows that ilmenite particles increased their reactivity as they were cyclically reduced and oxidized, especially during the initial 10–30 cycles. Afterwards, reactivity was still increasing, but with less intensity. However, the oxygen transport capacity also decreased during the redox cycles; see Fig. 10(b). To consider both factors, i.e. the variation of reactivity and R_{OC}, the changes in the oxygen transfer rate, r_O calculated by equation E(7), are plotted in Fig. 11(b).

As expected, the oxygen transfer rate also increased during the initial redox cycles. Interestingly, it was found that the oxygen transfer rate reached eventually a maximum value, which was roughly constant throughout the redox cycles. Considering this fact, the period characterized by the r_O increase is named as *"activation phase"*, whereas we refer as *"activated particles"* to the material having reached the maximum reaction rate. The number of cycles of the activation period depended on the reduction conversion reached in every cycle. Thus, the higher the reduction conversion, the lower number of cycles is needed to activate the ilmenite; see Fig. 12. In any case, the activation period is quite short considering the high number of cycles (hundreds or thousands) that the oxygen carrier must undergo in a chemical looping unit. Therefore, most of the particles in a chemical looping unit would be in the "activated" status.

The fact that the oxygen transfer rate was constant for the activated particles even when the oxygen transport capacity decreased is highly relevant for understanding the oxygen carrier kinetics. Thus, the same r_O value can be obtained from two activated particles with different oxygen

transport capacity. For example:

$$r_0 = \left|\frac{d\omega_0}{dt}\right| = R_{OC,1}\left|\frac{dX_{i,1}}{dt}\right| = R_{OC,2}\left|\frac{dX_{i,2}}{dt}\right| \tag{E8}$$

Note that even though the oxygen transfer rate was maintained constant for the activated particles, other properties such as porosity, crushing strength or oxygen transport capacity may vary with the redox cycles.

2.3.1. Kinetics of ilmenite particles

Ilmenite reactivity varies as it reacts in a chemical looping unit. Initially, ilmenite particles have a rather low reactivity with reacting gases, such as H_2, CO, CH_4, and O_2, and then reactivity increases during the activation period, until it reaches a constant value. Kinetics constants for both un-used or pre-oxidized particles and activated particles are available.

2.3.1.1. Kinetic model.
A reaction model of the ilmenite particles was considered for the reactions (R1)-(R8). Before considering any model for the reactions R1-R8 of ilmenite with the different reacting gases, it is necessary to highlight that from the conversion vs time curves determined in TGA it was not possible to distinguish the reduction of Fe_2TiO_5 from that of Fe_2O_3. Thus, a global kinetic rate constant was calculated for the sum of both reactions. Similarly, a global kinetic rate constant was obtained for the oxidation reaction. In this line, an average coefficient $\bar{b}$ was used.

SEM images showed a granular structure inside the ilmenite particles; see Fig. 9. Moreover, previous studies showed that the particle size in the range used in circulating fluidized beds did not affect the reaction
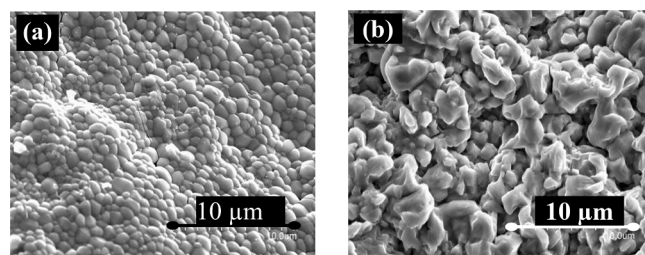

Fig. 7. SEM images of (a) pre-oxidized and (b) reacted ilmenite [40].

Table 5

Main properties of ilmenite particles, namely fresh, pre-oxidized and reacted in different facilities: TGA, batch fluidized bed reactor, 0.5 kW CLC unit and 1.5 kW CLG unit.

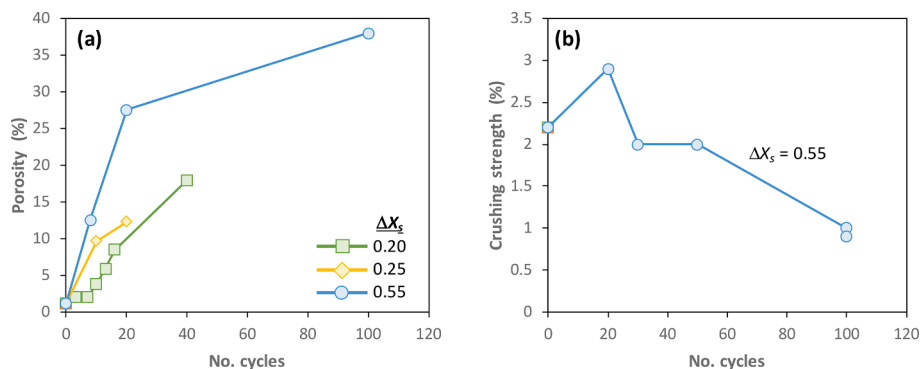|	Fresh	Pre-oxidized	Activated in TGA			Activated batch-FB CLC					Activated CLC unit	Activated CLG unit
Reference	[40]	[57]	[57]	[40]	[40]	[60]	[43]	[43]	[43]	[43]	[58 61 62]	[51]
ΔX_s during redox cycles			0.5	0.5	1.0	0.2–0.25	0.4	0.5	0.55	0.6	0.2	0.1–0.3
No. total redox cycles			30	100	10	16	23	20	100	20	60	150
No. redox cycles to be activated				30	4	7	20	10	10	4	40	
Oxygen transport capacity, R_{OC} (wt %)		4.0	3.3	2.1		3.9	3.5	3.3	2.1	2.9	3.9	3.8
Rate index (% min^{-1}, 1223 K)		H_2: 2.1 CO: 0.6 CH_4: 0.6 O_2: 4.8	H_2: 7.9 CO: 2.5 CH_4: 5.0 O_2: 9.8			H_2: 7.9 O_2: 9.8						
Porosity (%)	0	1.2	12.7	35		12.6		27.5	38.0		18	
Crushing strength (N)	2.4	2.2	2.0	1.0				2.9	1.0		2.0	
Skeletal density (kg m^{-3})	4580	4100	4250	4250				4220			4200	
BET surface (m^{2}g^{-1})	0.6	0.8	0.4	0.4			0.4	0.6	0.4			
Composition (wt.%)												
Fe_2O_3	14.8	11.2	22.0	39.0		11.5					11.7	
Fe_2TiO_5		54.7	38.5	12.0		54.0					53.2	
$FeTiO_3$	65.5					–						
TiO_2	14.0	28.6	34.0	43.5		29.5					29.5	
Inert	5.7	5.5	5.5	5.5							5.6	

Fig. 8. Variation of (a) porosity and (b) crushing strength with the redox cycles as a function of the variation of the solid conversion, ΔX_s. Ilmenite was fully oxidized in every redox cycle, i.e. CLC conditions [43].

rates of ilmenite. Therefore, the grain model with uniform reaction in the particle, controlled by chemical reaction, was used to describe the kinetics of ilmenite particles. The model assumes that the particle consists of a number of nonporous spherical grains of uniform radius, r_g. The reaction proceeds in the grain following the shrinking core model. Considering that the reaction is controlled by the reaction in the grain which corresponds to negligible resistances to gas film mass transfer and diffusion inside the particle, the equations that describe this model are the following:

$$\frac{t}{\tau_{chr}} = 1 - (1 - X_i)^{1/3} \quad \frac{dX_i}{dt} = \frac{3}{\tau_{chr}}(1 - X_i)^{2/3} \quad \text{(E9)}$$

The time to achieve complete conversion, τ_{chr}, is calculated as:

$$\tau_{chr} = \frac{\rho_m r_g}{b k_s C_{g,i}^n} \quad \text{10)}$$

The dependence on the temperature of the kinetic constant was assumed to be of Arrhenius type, as follows:

$$k_s = k_{s0} e^{-E_a/R_g T} \quad \text{11)}$$

To predict the behavior of the oxidation of calcined ilmenite a mixed resistance between chemical reaction and diffusion in the solid product was needed. This fact was likely due to the low porosity of calcined ilmenite. In this case, it was assumed that the reaction rate was controlled by chemical reaction in the grain up to a determined conversion value, X_{chr}, which will be determined from the conversion-time curves. During this period, the porosity of particles decreases because the molar volumes of the solid products ($Fe_2TiO_5 + TiO_2$ and Fe_2O_3) are higher than those for the solid reactants ($FeTiO_3$ and Fe_3O_4). This chemically controlled step proceeds until the porosity collapses. From this point, it was assumed that the oxidation proceeds following a

shrinking core model in the particle, and it is controlled by the diffusion in the solid. The equations that describe this oxidation step are the following

$$\frac{t}{\tau_{dif}} = 3\left[1 - \left(1 - X_0'\right)^{\frac{2}{3}} + \frac{1 - Z + (1 - Z)\left(1 - X_0'\right)^{\frac{2}{3}}}{Z - 1}\right] \quad \tau_{dif} = \frac{\rho_m R_p^2}{6\bar{b}D_e C_g} \quad \text{12)}$$

where Z is the expansion ratio between the solid product and solid reactive:

$$z = \frac{V_{m,prod}}{V_{m,reac}} \quad \text{13)}$$

and X_o' is a modified conversion that takes into account that the diffusional control starts at the conversion X_{chr}, and it is calculated as follows:

$$X_0' = \frac{X_0 - X_{chr}}{1 - X_{chr}} \quad \text{14)}$$

being $X_o' = 0$ at $X_o = X_{chr}$, and $X_o' = 1$ at $X_o = 1$.

The time necessary to reach any conversion for values higher than X_{chr} is given by

$$t = t_{dif} + t_{chr}|X_{chr} \quad \text{15)}$$

The values of the kinetic parameters obtained for the reduction and oxidation of pre-oxidized and activated ilmenite are given in Table 6.

Although kinetic parameters for pre-oxidized and activated particles are available in the literature, for practical purposes, the kinetics determined for the activated particles are valid to characterize the reactivity of ilmenite particles in a chemical looping unit [57]. This is justified due to the reactivity increases during the initial hours of operation until activated state is quickly achieved. Then, the oxygen
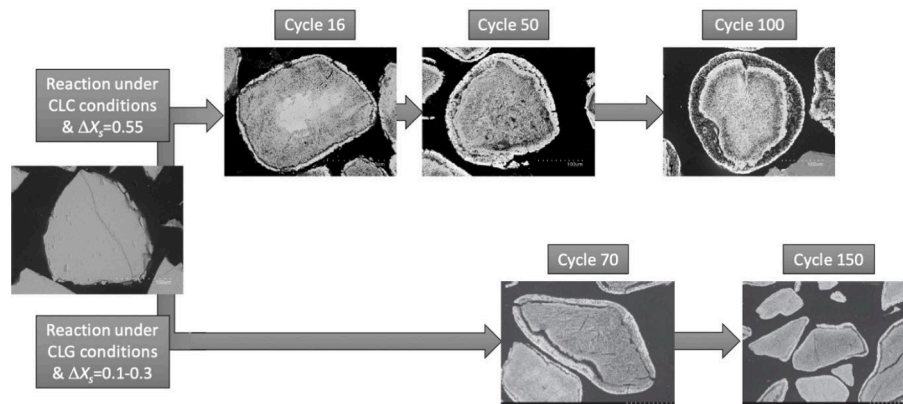

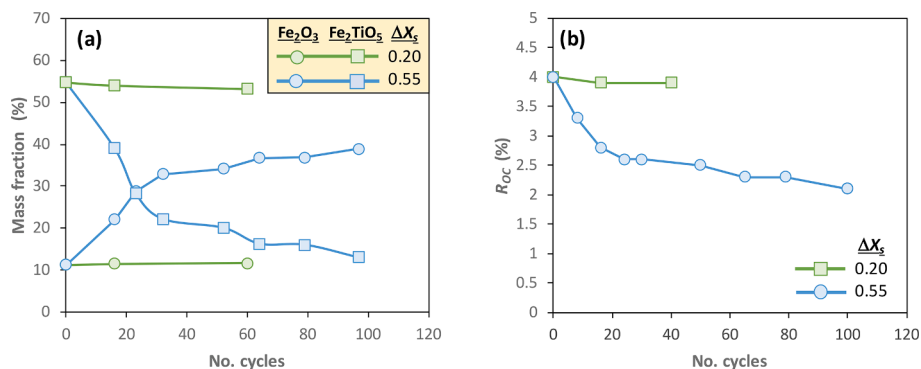**Fig. 9.** SEM image of the fresh and used ilmenite particles under CLC and CLG conditions [43,51].

Fig. 10. Changes in (a) the mass fraction of Fe_2TiO_5 and Fe_2O_3 in ilmenite particles and (b) the oxygen transport capacity, R_{OC}, during redox cycles under CLC conditions for values of the variation of the solids conversion, ΔX_s, of 0.2 and 0.55 [43].
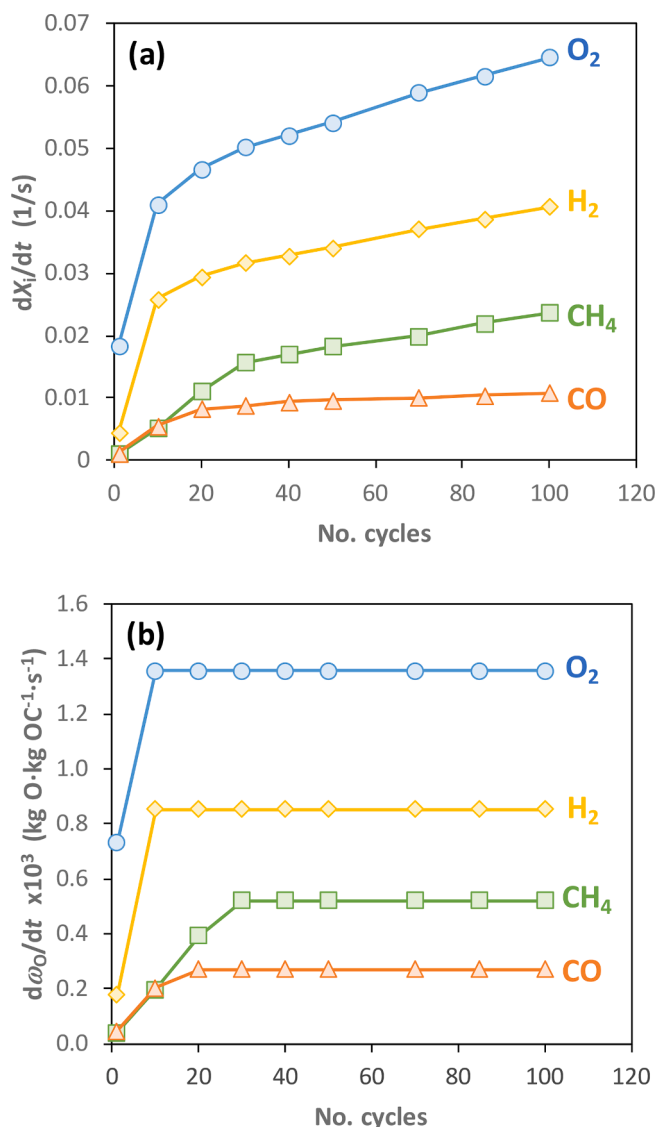

The kinetic parameters for the reduction –with H_2, CO and CH_4– and oxidation reactions of activated ilmenite were obtained using particles with a value of the oxygen transport capacity of $R_{OC} = 0.033$ [57]. This value, as well as dX_i/dt, may vary depending on the number of redox cycles and the ΔX_s value in each redox cycle; see Fig. 10(b) and 11(a). However, the property shown in equation (E.8) can be used to apply the kinetics previously determined to any condition for activated ilmenite particles. This property considers that the same oxygen transfer rate, r_O, can be obtained from two activated particles with different oxygen transport capacities. Although the oxygen transport capacity of ilmenite particles could decrease with the operating time, it was observed that the oxygen transfer rate remains constant after activation. Therefore, equation (E.8) is used to calculate the reactivity of activated ilmenite particles. From the kinetics showed in this work, the value of $(dX/dt)_1$ can be calculated for activated ilmenite particles which has a value of $R_{OC,1} = 3.3$ wt%. According to equation (E.8), at each oxygen transport capacity of activated ilmenite, $R_{OC,2}$, a value for reactivity $(dX/dt)_2$ can be calculated to be used for modelling purposes.

2.4. Reaction kinetics of ilmenite at pressurized conditions

Most of the know-how developed up to date on CLC is based on operation at atmospheric pressure. However, chemical looping technologies at pressurized conditions have the potential of increasing the overall energy efficiency of the processes since gas turbine technology could be used in combined cycles to achieve higher values of electric efficiency and lower amounts of additional compression power for CCS would be required [64,65]. Operating at pressurized conditions, the fuel flow fed into the fuel reactor dramatically increases, whereas the amount of oxygen present in the oxygen carrier particles is constant. Thus, it is critical to have oxygen carriers that exhibit a suitable performance in terms of reactivity, when they operate at pressurized conditions [66].

In the particular case of ilmenite, CanmetENERGY-Ottawa has extensively studied the reactivity of this material for redox reactions at pressurized conditions with a wide range of gaseous fuels. In this regard, this research group analyzed the reduction kinetics of an upgraded roasted natural ilmenite ore for Pressurized Chemical Looping Combustion of CH_4 [67] and a simulated natural gas [68] in a pressurized thermogravimetric analyzer (PTGA). In the former case, the fuel gas mixture was composed of CH_4 and CO_2 (N_2 to balance), whereas in the latter case small amounts of C_2H_6 and C_3H_8 were also added. In both cases, the same ranges of total pressure (0.6–1.6 MPa) and methane partial pressure (0.23–0.64 MPa) were studied, and the same Hancock and Sharp method was used to establish the kinetic models for ilmenite reduction. The main conclusions were similar in both studies: 1) an increase of the CO_2 partial pressure and the total pressure reduced the rate of conversion during ilmenite ore reduction; 2) the ilmenite conversion rate had a strong positive correlation with the fuel partial pressure.

Fig. 11. Evolution with the redox cycles of (a) reactivity defined as dX_i/dt and (b) oxygen transfer rate, $r_O = d\omega_o/dt$, for reaction with 15 vol% of CO, H_2 or CH_4 and 10 % O_2. CLC conditions with $\Delta X_s = 0.55$ and $T = 1173$ K [40].

transfer rate, characterized by the *Rate index*, was maintained constant; see Fig. 11(b). This fact implies that most of ilmenite particles being used as oxygen carrier in a chemical looping unit are completely activated.
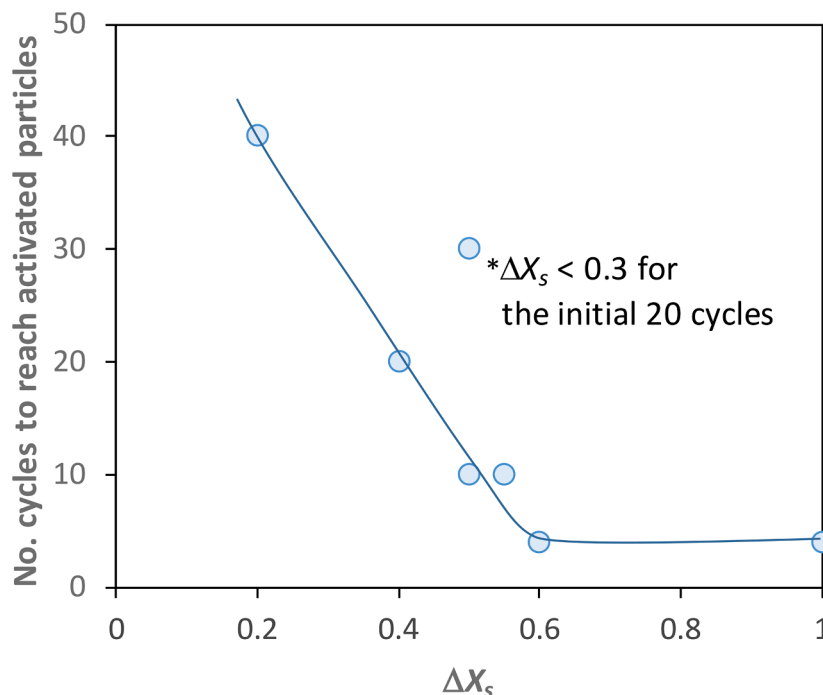
Fig. 12. Number of redox cycles required to achieve activated ilmenite particles as a function of the variation of the solids conversion in each cycle, ΔX_s.

Furthermore, they studied the reactivity of ilmenite with sour gas in a PTGA at pressures up to 4 bar (a) and they observed that the presence of H_2S (up to 3030 vppm) had a positive effect on the reactivity of ilmenite for both the reduction and the oxidation steps [68].

Similar results to those obtained with CH_4 and natural gas were achieved using CO as fuel. In this regard, Lu et al. [69] concluded that higher reaction rates were achieved when the CO partial pressure was increased maintaining constant the total pressure in the PTGA. On the contrary, increasing the total pressure at a constant CO partial pressure resulted in a slower reduction rate. Ridha et al. [42] carried out a comprehensive characterization of the ilmenite samples subjected to the redox cycles discussed above using CO as a reducing agent. SEM results confirmed that the surface morphology of aging ilmenite ore particles was unaltered despite operating at total pressures of up to 51 bar and with CO partial pressures between 3.2 and 8.0 bar.

The results obtained by Lu et al. [69] were in disagreement with the conclusions found by Zaabout et al. [70] from SINTEF, who observed that an increase in total pressure from 1 bar to 5 bar slightly improved CO conversion using ilmenite as an oxygen carrier. These experiments were not conducted in a PTGA, but in a larger facility, that is, in a lab-scale fluidized bed reactor for the Gas Switching Combustion (GSC) process.

Regarding oxidation kinetics of ilmenite at pressurized conditions, Rana et al. [71] performed a series of experiments in a PTGA varying the partial pressure of O_2 between 0.2 bar and 1.6 bar at a total pressure of 8 bar. The total pressure was also changed from atmospheric pressure to 16 bar using pure air as oxidizing agent. The reaction rate decreased as total pressure increased when maintaining a constant O_2 partial pressure. On the contrary, total pressure had a positive effect on the rate of the oxidation reaction with a constant O_2 volume fraction. These authors also evaluated the effect of pressure on the mechanical integrity of the ilmenite particles and observed that high O_2 partial pressures had a negative effect due to fragmentation phenomenon whereas low O_2 partial pressures favored the migration of iron oxide to the surface of the particles.

3. Use of ilmenite with different processes and fuels: gaseous, liquid and solids

3.1. Use of ilmenite in OCAC

Fluidized beds are characterized by exhibiting good mixing properties. However, there can be localized regions where there is insufficient oxygen to fully combust the fuel. This is where the Oxygen Carrier Aided Combustion (OCAC) process emerges. It consists in replacing totally or partly the inert bed material, typically silica sand, by oxygen carrying metal oxides with the aim of increasing the oxygen distribution in the reactor, see Fig. 13.

We see that the oxygen carrier is transported in the freeboard by the flow entering the reactor. The freeboard is a highly reactive zone where the oxygen carrier can react with the fuel transferring its oxygen content to it. In this way, oxygen is available to convert the fuel also in areas of the reactor which are distant from the inlet of primary air. On the other hand, the oxygen carrier which has reacted is obviously reduced and so it enters the cyclone and it is recirculated to the bottom of the reactor where it enters in contact with air again and it is oxidized once again. In this way, the redox cycle of the oxygen carrier is restarted.

Using oxygen carriers as bed materials may improve the combustion efficiency of the process and reduce the hotspots because of its buffering ability [72–74]. Additionally, the use of oxygen carriers may contribute to decrease the excess oxygen, resulting in lower operating costs. Oxygen carriers are capable of transferring oxygen to the fuel in lean oxygen zones and oxidizing/regenerating in rich oxygen zones of the reactor. Therefore, the OCAC process stems from the chemical looping combustion concept except that oxidation and reduction of the oxygen carrier take place in the same reactor. Of course, CO_2 capture is not inherent to the OCAC process, as it is the case of CLC because here the combustion process is split in two reactors. Many research studies have been carried out by using ilmenite as bed material since it has exhibited high reactivity with CO and H_2 in continuous CLC processes when burning solid fuels both at lab-scale and industrial scale [72]. Fig. 14 shows a scheme of the 12 MW_{th} boiler reactor system at Chalmers University and Fig. 15 reports the industrial development of OCAC at this institution.

Table 6

Kinetic parameters for ilmenite reduction (H_2, CO and CH_4) and oxidation (O_2).

Kinetic parameters	H_2		CO		CH_4		O_2	
	Calcined	Activated	Calcined	Activated	Calcined	Activated	Calcined	Activated
ρ_m (mol/m^{-3})	13,590	13,590	13,590	13,590	13,590	13,590	31,100	31,100
r_g (m)	$0.5\ 10^{-6}$	$1.25\ 10^{-6}$	$0.5\ 10^{-6}$	$1.25\ 10^{-6}$	$0.5\ 10^{-6}$	$1.25\ 10^{-6}$	$0.48\ 10^{-6}$	$1.20\ 10^{-6}$
$\bar{b}$	1.19	1.45	1.19	1.45	4.74	5.78	4	4
k_{s0} (mol^{1-n} m^{3n-2} s^{-1})	$5.1\ 10^{-1}$	$6.2\cdot10^{-2}$	$2.1\ 10^{-1}$	$1.0\cdot10^{-1}$	8.8	9.8	$8.0\cdot10^{-5}$	$1.9\cdot10^{-3}$
E_{ks} (kJ/mol)	109.2	65.0	113.3	80.7	165.2	135.2	11.8	25.5
n	1	1	1	0.8	1	1	1	1
$D_{0,e}$ (mol/m$^{-2}(-|-)$ s^{-1})							$1.37\cdot10^{-5}$	
E_{De} (kJ/mol)							77.4	

Zhao et al. [76] run tests in a lab-scale batch fluidized bed combustor. In this case, a mass fraction of 40 % of ilmenite in silica sand was used. The experimental tests were performed by introducing different wood char loads into the reactor in order to simulate different air to fuel ratios. They stated that there was a beneficial effect on the fuel conversion when using ilmenite as bed material, instead of silica sand, based on the CO_2 yield. Chadeesingh and Hayhurst [77] performed experimental tests in a lab-scale fluidized bed combustor adding different amounts of Fe_2O_3 into a sand bed supplying CH_4 as fuel. They observed that the addition of Fe_2O_3 enhanced the CH_4 combustion at 700 °C. Schneider et al. [78] carried out a detailed studied of CH_4 combustion in a bubbling fluidized bed using ilmenite and silica sand as bed materials by the measurement of the product gas along the reactor height. They found that the use of ilmenite as a bed material enhances the CO_2 yield in the fluidized bed itself significantly compared to silica sand, in which an abrupt combustion was detected in the freeboard gas phase.

Recent results obtained by Garcia et al. [79] in a 30 kW$_{th}$ coal fired FB are also in line with other authors findings. A reduction of excess air to achieve complete combustion and lower efficiency loss compared to silica sand were found.

Regarding the implementation of OCAC in industrial facilities, some tests in a 12 MW CFBC burning biomass were conducted in OCAC mode. Silica sand was gradually replaced by ilmenite, up to 40 wt%. They observed that operating with ilmenite as bed material, CO and NO emissions decreased by 80 % and 30 %, respectively, compared to silica sand tests. Moreover, a lower profile temperature in the cyclone was noticed, which suggested an improved oxygen distribution in the reactor.

During the last years, the utility company E.ON and Chalmers University of Technology have collaborated to develop the OCAC concept to industrial applicability [75]. A 75 MW$_{th}$ CFB E.ONś Boiler 14 located in Norrköping (Sweden) was operated during 4000 h burning Municipal Solid Waste (MSW) and using ilmenite as bed material, see Fig. 16. It was observed that the flue gas became less prone to cause fouling on the heat transfer surfaces in the boiler back pass and lower average of CO emissions and more consistent values were achieved operating with ilmenite. Less peaks of CO during operation were registered by analyzers, which demonstrated the buffering ability of the oxygen carrier.

Moldenhauer et al. [80] obtained interesting results during the operation of a 115 MW$_{th}$ biomass fired CFB boiler with ilmenite as bed material. The experiments showed that (1) it was possible to swap silica-sand for ilmenite without making variations to existing equipment and (2) that the external and internal bed material logistics works equally well. Ilmenite improved the oxygen distribution in the furnace, which led to a reduction of the air surplus by as much as 30 % and an increase of the net boiler load from 115 MW$_{th}$ to 123 MW$_{th}$. The experiment showed that average NO$_x$ concentrations and ammonia consumption tend to be higher, compared to silica-sand operation.

Moreover, in view of the promising results obtained in OCAC under air combustion conditions, CanmetENERGY-Ottawa contemplated the use of this new concept to oxy-fuel FB boilers. In oxy-fired units designed for carbon capture and storage, reducing the excess oxygen requirement is even more important than in conventional air combustion. Typically, the oxygen is produced using a cryogenic air separation unit (ASU) which has both a large power requirement and high capital cost. Reducing excess oxygen decreases the consumption of oxygen that is unnecessary to achieve complete combustion. Hughes et al. [81] extended the OCAC research work to include testing under oxy-fired conditions using a 50 kW$_{th}$ Bubbling FB pilot-scale boiler with two Canadian coals. Similar results to those achieved under air-fired conditions were obtained, i.e, CO emissions were reduced by using ilmenite ore as the bed material. This improvement was more significant when the flue gas excess O_2 was < 3 vol% (dry basis) and/or operating at low bed temperatures (800 °C). de las Obras Loscertales et al. [82] conducted tests in the same 50 kW$_{th}$ pilot-plant operating in CFBC configuration with torrefied biomass. Good results, similar to those obtained under the bubbling FB configuration, were achieved with respect to CO emissions and oxygen excess. Therefore, the novel OCAC concept is a promising process that may be suitable for operation in both oxy-BFB and CFBC configurations.

The OCAC concept has also been considered as an approach for hydrogen production. Stenberg et al. [83] explored the integration of steam methane reforming with oxygen carrier aided combustion using Aspen Plus. The simulation showed that a reduction in the required flue gas temperature and a lower required air excess led to a decrease in the methane consumption in a system with only small modifications compared to conventional processes.

Ageing of ilmenite particle in OCAC has been studied, and some results may be of interest to improve the confidence level for its use in CLC/CLG. Corcoran et al. [84] also analyzed the physical properties of two distinct ilmenites: sand ilmenite and rock ilmenite. They observed that both materials differed in their structural development, which affected their corresponding mechanical stability. Two different mechanisms were suggested for the material degradation. It was noticed that the sand ilmenite was shattered into numerous small pieces, whereas the rock ilmenite was divided by the cracks formed. Likewise, two pathways of elemental distribution development of iron in the oxygen carrier particles over the exposure time in OCAC mode were found for the two types of ilmenites. In both cases, the iron had migrated to areas with high oxygen potential. The sand ilmenite developed cavities inside the particles in which the iron migrated. For the rock ilmenite, on the contrary, the iron was migrated to the surfaces of the particles [85].

In addition to the changes in the solids derived from the redox processes, solid fuel combustion in FBCs may present issues related to ash composition (K, Ca, etc) such as corrosion of the heat transfer equipment and, agglomeration or sintering of the bed material causing defluidization and thus the disruption of the operation. Zevenhoven et al. [86] carried out agglomeration tests in a lab-scale fluidized bed reactor to analyze the influence of potassium-containing components on ilmenite ore as bed material. In this work, pure salts (KCl, KH_2PO_4, K_2CO_3 and K_2SO_4) were added into the combustor. They found that the main responsible for defluidization of the bed material were KCl, KH_2PO_4 and K_2CO_3. KCl and KH_2PO_4 caused agglomeration by gluing particles
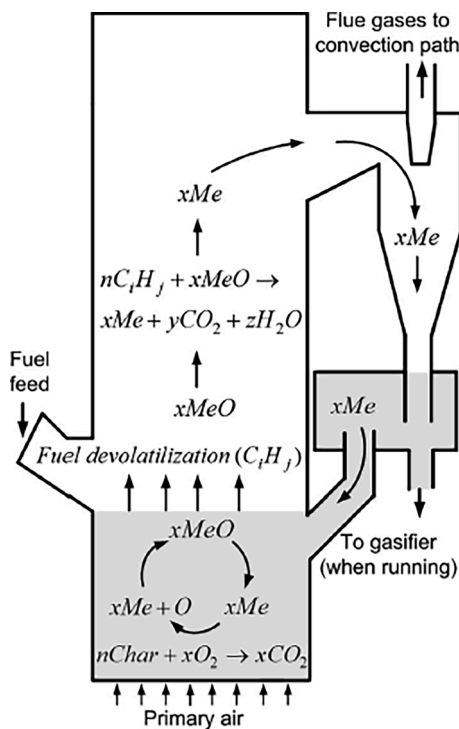
Fig. 13. Layout of an OCAC plant [72].

Fig. 15. Development of industrial application of OCAC at Chalmers university [72,75].

agglomeration of ilmenite bed particles. Corcoran et al. [87] studied the ash properties of ilmenite when it was mixed (40 wt%) with silica sand as bed material in a 12 MW CFBC. They found that iron from ilmenite segregated to the surface, whereas titanium remained in the core of the particle. It was observed that potassium diffused toward the core of the ilmenite particle forming the compound KTi_8O_{16} and calcium appeared as a double layer surrounding the iron of the particle. The fact that potassium was in the inner part of the particle might be a key factor to solve or reduce agglomeration and corrosion issues. Experimental tests in a 30 kW_{th} coal fired FB revealed that ilmenite could hinder the K-rich molten substance attachment to the bed material, leading to significantly smaller agglomerates and hence less tendency towards defluidization in comparison to silica sand [79].

Recently, Stanicic et al. [88] analyzed the interaction of metal traces (Cu, Zn and Pb) with ilmenite of several samples taken from two waste fuel-fired CFB plants of 115 MW_{th} and 75 MW_{th}. They found that lead interacted with titanium forming $PbTiO_3$, whereas zinc and copper interacted with the iron from ilmenite forming the $CuFe_2O_4$ and

together. However, because of the high temperatures used in OCAC systems, it is expected that most KCl be vaporized and thus not representing a problem for OCAC systems. K_2CO_3 reacted with the ilmenite to form a potassium titanate leading to agglomeration at temperatures above 950 °C. Additionally, K_2SO_4 addition resulted in no
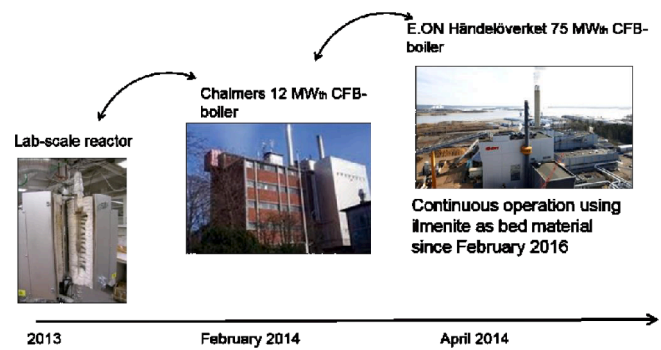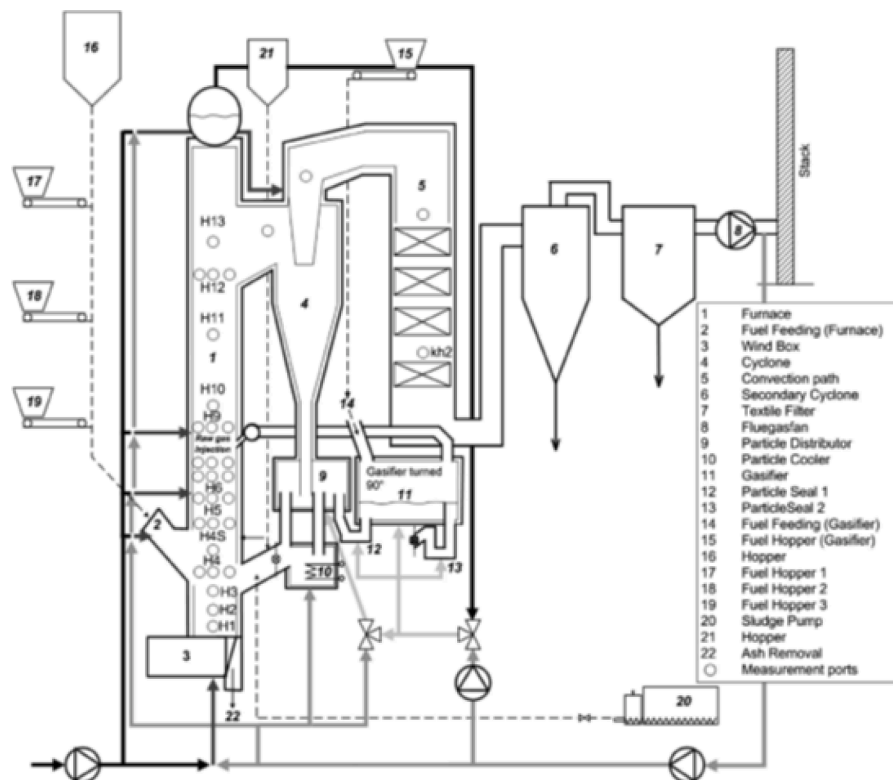

Fig. 14. The 12 MW_{th} Chalmers boiler reactor system [72].

ZnFe$_2$O$_4$ ferrites. This fact could also assist in minimizing corrosion issues in the heat transfer surfaces and in making ash less hazardous for further disposal.

Further studies performed in the 75 MW$_{th}$ CFB boiler by Lind [89] demonstrated the industrial implementation of OCAC process with over 12,000 h of operation using ilmenite as bed material. In conventional FBCs, the silica sand bed is regenerated excessively in order to prevent agglomeration issues so that the price of the material together with the market availability logistic and operational costs become a key factor in the development of the OCAC. The fact that ilmenite contributes to decrease agglomeration and corrosion issues may affect the regeneration rate of bed material needed in the combustor. Gyllén et al. [90] suggested the installation of a magnetic separator to send back spent ilmenite into the boiler since after being exposed to OCAC conditions, ilmenite could be magnetically separated, lowering operational costs.

3.2. Use of ilmenite in chemical looping combustion

Ilmenite has very good performance in Chemical Looping Combustion thanks to its important stability and reactivity. In the following sections the behavior of ilmenite with solid fuels, gaseous fuels and liquid fuels are presented.

3.2.1. Solid fuels

The most comprehensive review regarding the use of ilmenite as oxygen carrier for the combustion solid fuels was performed by Adánez et al. [18]. Table 7 shows an overview of the most relevant results obtained in continuous CLC units using solid fuels with ilmenite as oxygen carrier. Fig. 17 shows the general scheme of the 1MW$_{th}$ CLC pilot plant located in Darmstadt, being the largest CLC plant built for solids fuels up to date.

The use of Chemical Looping technologies burning biofuels allows achieving negative CO$_2$ emissions. Next, two relevant research works performed in large-scale pilot plants using ilmenite as oxygen carrier to burn biofuels are listed. An experimental campaign at VTT Technical Research Center of Finland in a 20 kW$_{th}$ CLC prototype burning biomass with ilmenite was carried out [107]. Furthermore, experimental tests were conducted at Chalmers University, using the boiler/gasifier loop (with inputs of 12 MW$_{th}$ and 2–4MW$_{th}$, respectively) during more than 1000 h of operation with ilmenite and a manganese ore as oxygen carriers and commercial wood pellets from spruce trees as fuel. [108]. The results demonstrated that ilmenite sand is a suitable oxygen carrier material for large-scale operation of CLC units, as it effectively transported oxygen from the combustor to the fuel reactor.

3.2.2. Liquid fuels

The experience of the use of ilmenite with liquid fuels in CLC processes is very limited. Until 2019, only 150 h of operation had been carried out in continuous pilot plants using kerosene [109], diesel [110] and heavy fuel oil [111] as fuels. In the work of Moldenhauer et al. [109] a 300 W lab-unit reactor was used to burn kerosene in a chemical looping process. The fuel reactor was fluidized by a steam-fuel mixture. This process facilitates the injection of the fuel in the fuel reactor, in fact superheated steam is used to vaporize the fuel and lead it inside the reactor. In this way the injectors which are designed to be used with gaseous fuels can be used also for the mixture of steam-kerosene without the need of any adaptation. Given the above-said configuration it is clear that the reactions inside the fuel reactor were not only related to the oxidation of the fuel but also related to the steam reforming of the hydrocarbons. The carbon conversion to CO$_2$ reached 84 % when the fuel consumption per second was about 143 W$_{th}$. The remaining gases were CO and H$_2$ which were originated from the reforming reactions and
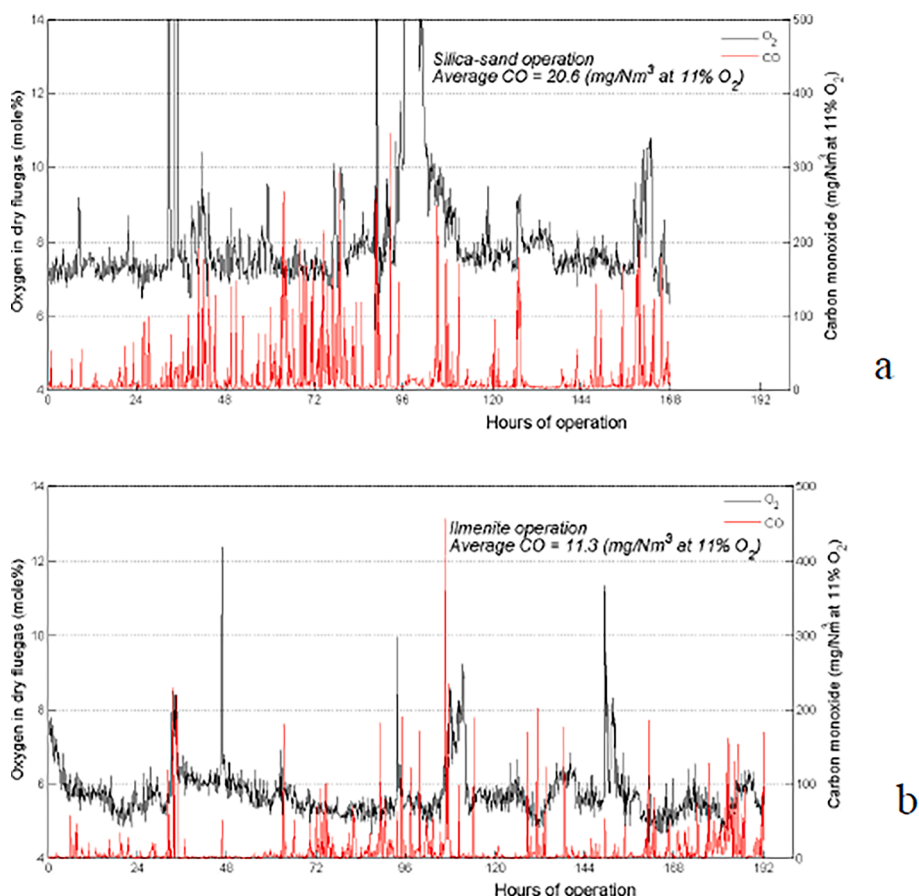
Fig. 16. Operation using, a) silica-sand as bed material and operation using, b) a mix of ilmenite and silica-sand as bedmaterial in a 75 MW$_{th}$ CFB boiler [75].

increased their concentrations as temperature increased. Changing the fuel to high-sulfur kerosene significantly increased CO_2 yield up to 99 %, see Fig. 18. Besides, it was noted that the reactivity of ilmenite considerably increased throughout the successive redox cycles.

Successful experiments were performed using ilmenite as oxygen-carrier and diesel as fuel [106]. Fuel addition took place during almost 67 h and the oxygen carrier was fluidized at hot conditions for more than 200 h. A temperature interval of 900–1050 °C was tested at a varied circulation of solids. The fuel input was varied between 4 kW_{th} and 6 kW_{th}, which corresponded to an oxygen carrier-to-fuel ratio in the fuel reactor that ranged from 1400 to 2100 kg/MW_{th}. At 1050 °C and a fuel flow corresponding to 4 kW_{th}, the fuel could be oxidized to about 87 % and up to 88 % of all carbon leaving the fuel reactor was in the form of CO_2. Furthermore, carbon leakage to the air reactor was very low and close to the detection limit. The mechanical integrity of the ilmenite particles was adequate and no noteworthy problems, such as high attrition rate, agglomeration of bed material, or defluidization, were encountered.

Finally, 4 h of operation were conducted in a 10 kW_{th} CLC unit with ilmenite using a heavy fuel oil as fuel [107]. The experiments were carried out with a fuel flow corresponding to 4.0–6.2 kW_{th} and an oxygen carrier-to-fuel ratio of about 1300–2000 kg/MW_{th}. The highest degree of fuel oxidation was just below 87 % and was achieved at a temperature of 950 °C. Regarding the effect of sulfur present in the fuel on the performance of ilmenite it could be concluded that sulfur was not accumulated in the oxygen carrier particles and therefore the material was not deactivated. Most of the sulfur was detected in the gas phase in the form of H_2S.

3.2.3. Gaseous fuels

In the work of Jerndal et al. [112] the activity of ilmenite is interestingly compared with that of other oxygen carriers to understand its performance with syngas. For the screening of the oxygen carriers a quartz reactor was used with a height of 870 mm and an inner diameter of 22 mm. The bed was prepared by mixing 3 g of oxygen carrier with 12 g of inert quartz. The particles in the bed had a diameter comprised between 125 and 180 μm. The temperature of the reactor was set at 950 °C. The oxygen carrier was chosen in a small quantity and represented about 20 % in weight of the total bed mass because it was desired to achieve incomplete conversion of the gas to compare the selected oxygen carriers. The syngas used had a ratio of 1:1 in volume for carbon monoxide and hydrogen. Ten low-cost Fe-based oxygen carriers were selected. Seven of these materials were oxide scales provided by different suppliers, like SCANA, Sandvik and ESAB. The other three oxygen carriers were the following: an industrial iron material from Höganäs, an iron ore from KLAB, and an iron material produced from the vehicle recycling company Stena Metal. These oxygen carriers were compared with ilmenite as reference. The conclusion of this work was that ilmenite resulted to be less reactive than the majority of the selected low-cost oxygen carriers with both carbon monoxide and hydrogen [112]. Another very interesting characteristic of this scrap metals was that some of them had a very high crushing strength (about 11 N) compared to ilmenite (about 4.0 N). In the work of Leion et al. [6] the reactivity of Fe- and Mn-based ores and industrial products was evaluated using syngas and methane as fuels. Colormax EF, SSAB Röd, and ilmenite met all criteria presented in this work and should be suitable oxygen carriers. The conversion of carbon into CO_2 approached 100 % for the three above mentioned oxygen carriers. From the experiments performed by Leion et al. [4] it could be concluded that reactivity between ilmenite and syngas is good whereas reactivity with methane is lower if it is compared to the that exhibited by other oxygen carriers [4]. In the work of Bidwe et al. [113] a 10 kW_{th} dual fluidized bed plant was used to carry out syngas conversion tests and CO and H_2 conversion values close to 90 % were achieved. The excellent performance of ilmenite in terms of H_2 conversion was also confirmed by Kolbitsch et al. [114], who achieved values comprised between 90 and 95 % in a 120

kW_{th} dual fluidized bed reactor. A dual fluidized bed reactor configuration was also considered by Tsinghua University [115], see Fig. 19, to perform CLC combustion tests with ilmenite as oxygen carrier.

The plant was operated for 100 h using carbon monoxide as reducing gas. The reaction temperature was maintained at 900 °C. The best performance was exhibited by a K^+ promoted ilmenite reaching CO conversion values between 89 % and 100 %.

3.3. Use of ilmenite in chemical looping reforming

Chemical Looping reforming (CLR) is one of the most promising technologies for the production of synthesis gas, or syngas, with reduced CO_2 emissions. This syngas is an essential raw material for a wide variety of industrial processes such as gas-to-liquids (GtL) conversion, and the production of hydrogen, ammonia and methanol [36]. In an autothermal chemical looping reforming process (a-CLR, or simply CLR) the oxygen-to-fuel ratio is low in order to avoid the complete oxidation of the fuel to CO_2 and H_2O. Thus, a partial oxidation of the fuel is achieved in order to have a gas stream concentrated in CO and H_2. To obtain a gas undiluted in N_2 and with high heat value, the partial oxidation is usually done using O_2 instead air. However, in CLR the Air Separation Unit (ASU) required in the conventional auto-thermal reforming is not necessary.

The main oxygen carriers used to date in CLR processes are those based on nickel oxide due to the excellent catalytic properties of this metal for steam methane reforming reaction [8,116]. In the specific case of ilmenite, few studies have considered the use of this material as oxygen carrier for CLR. Recently, synthetic iron titanates have been identified as very promising materials for use in CLR. Prof. Liang-Shih Fan's group at The Ohio State University (OSU) has developed a co-current moving bed gas–solid contact pattern coupled with iron-–titanium composite metal oxide (ITCMO) carriers to produce high purity syngas for chemicals production applications such as dimethyl-ether or gasoline and diesel through a GtL process using shale gas [117], natural gas [118], and mixtures of $CH_4/CO_2/H_2O$ [119,120] or CH_4/coal [121] as fuels. Furthermore, Karimi et al. [122] studied the behavior of an oxygen carrier based on iron oxide, supported on TiO_2 and prepared by the precipitation method for the production of hydrogen through CLR in a fixed-bed reactor in a range of temperatures between 700 and 1200 °C reaching a maximum fuel conversion of 80 %.

Regarding the use of naturally occurring ilmenite ores, the research group of CanmetENERGY-Ottawa led by Dr. Robin Hughes has studied the use of an upgraded Canadian ilmenite ore as oxygen carrier for the production of syngas, heat, power and steam generation for diluent production at steam assisted gravity drainage (SAGD) facilities through pressurized chemical looping reforming (PCLR) technology [36]. Experimental testing in a fixed-bed reactor together with a detailed characterization of the ageing ilmenite particles determined the optimal operating regime to obtain a high quality syngas suitable for GtL processes. These experimental results were used to carry out the material and heat balances by means of Aspen Hysys V9 process simulation software of an entire PCLR process for SAGD applications. The energy balance showed that all the SAGD power and steam requirements could be met from a portion of the syngas steam destined to the GtL process while considerably reducing the CO_2 emissions into the atmosphere. This research group also studied the effect of the presence of CO_2 in the natural gas stream for the CLR process with ilmenite and they found that this compound considerably hinders the reduction of the iron species present in the mineral beyond Fe^{2+}, a reaction that is essential for the production of syngas. This issue was tried to be solved by adding NiO to the ilmenite particles, which not only allowed the production of a high quality syngas through the partial oxidation of CH_4 in the presence of CO_2, but also significantly improved the reactivity of this NiO-modified ilmenite ore oxygen carrier [123].

Table 7
Summary of the main results obtained in continuous CLC units using solid fuels with ilmenite as oxygen carrier.

No.	Name	Nominal power (kW)	OC	Fuel	FR design	T (°C)	φ	m_{OC} (kg/MW$_{th}$)	X_{sf} (%)	Carbon capture		Oxygen demand		Ref.
										η_{CC} (%)	χ_{OO} (%)	Ω_{FR} (%)	Ω_T (%)	
1	CUT	10	Ilmenite	Bit. Coal	Bubbling	950	0.5–2.2	1850–2940	50–80	82.5–96	83–93	16–22	n.a.	[91]
2	CUT	10	Ilmenite	Petcoke	Bubbling	950	0.4–1	1030	66–78	60–75	n.a.	~ 25	n.a.	[92]
3	CUT	10	Ilmenite	Petcoke	Bubbling	950–1000	0.5–1.5	1117	55–75	68–87	n.a.	27–36	n.a.	[93]
4	CUT	10	Ilmenite + CaCO$_3$	Petcoke	Bubbling	950–1000	0.7–2.5	1430	41–81	58–86	64–81	24–33	n.a.	[94]
5	CUT	10[a]	Ilmenite	Bit. Coal	Bubbling	970	1.5–8	2000	54–56	90–95	88–92	23	n.a.	[95]
6	CUT	10[a]	Ilmenite	Petcoke	Bubbling	970–1000	0.5–3.8	1364	45–65	51–87	61–83	18–21	n.a.	[95]
7	CUT	100	Ilmenite	Bit. Coal	High vel.	970–1000	1–5	200–770	52–67	n.a.	96–99.5	16–25	n.a.	[96,97]
8	CUT	100	Ilmenite	Wood char	High vel.	940–980	1–6	300–850	54–89	n.a.	91–97	4.7–15.5	n.a.	[98]
9	CUT	100	Ilmenite + Mn ore	Bit. Coal	High vel.	929–973	0.5–3	370–1300	54–77	n.a	98–99	8.5–18.5	n.a.	[99]
10	ICB-CSIC	0.5	Ilmenite	Bit. Coal	Bubbling	935–971	1.1	3140	95	35–86	n.a.	5–15	5–10	[100]
11	ICB-CSIC	0.5	Ilmenite	Bit. Coal	Bubbling	890	0.5–8.4	1500–3900	80–95	38–74	n.a.	14–36	8–15	[61]
12	ICB-CSIC	0.5	Ilmenite	Bit. Coal	Bubbling	850–920	1.0	1380	77	41–55	n.a.	~ 25	~ 9.5	[101]
13	ICB-CSIC	0.5	Ilmenite	Lignite	Bubbling	870–920	1.2	1770	89	82–93	n.a.	29–31	7–8	[101]
14	ICB-CSIC	0.5	Ilmenite	Anthracite	Bubbling	870–930	1.0	1400	87	20–40	n.a.	~ 16	~ 3.5	[101]
15	ICB-CSIC	50	Ilmenite	Bit. Coal	High vel.	905–1006	1.1–1.5	253–680	80–94	61–90	n.a.	8–14	6.5–9.8	[102,103]
16	TUHH	25	Ilmenite	Lignite	2 reactors	900–940	16–55	4505[c]	92	96–98	n.a.	11–25	10–24	[104]
17	TUD	1000	Ilmenite	Bit. Coal	High vel.	930	1	156	n.a.	n.a.	n.a.	12–17[b]	n.a.	[105]
18	TUD	1000	Ilmenite	Anthracite	High vel.	900	1.6	100	50	90	n.a.	20	n.a.	[106]

[a] : In-bed coal feeding.
[b] : Fuel reactor was fluidized with a mixture of air and steam.
[c] : Solids inventory per fuel reactor stage.

3.3.1. Chemical looping tar reforming (CLTR)

Since 2013 the works of Lind et al. [124] have shown promising results in the development of a new concept of biomass Chemical Looping Reforming. This is an extremely interesting technology given the great attention that the bioenergy sector paid to the coupling of reforming processes to pyrolysis. For example, it can be considered the Thermo-catalytic Reforming (TCR) process developed at Fraunhofer UMSICHT, Fraunhofer Institute for Environmental, Safety, and Energy Technology, Sulzbach-Rosenberg by prof. Hornung [125] or the experiments on catalytic reforming of biomass performed at the University of the Basque Country by the group of prof. Bilbao [126] with different reactor configurations such as spouted bed reactors.

In the practical case, the process proposed at Chalmers is based on an intelligent way to regenerate the catalyst (in this case ilmenite as oxygen carrier) via chemical looping, see Fig. 20.

The concept is better explained in the research work performed by Lind et al. [127] where the process is demonstrated by an initial experiment with producer gas from the Chalmers biomass gasifier using ilmenite (FeTiO$_3$) as catalytic bed material. The tar cleaning system was operated at 800 °C and fed with raw gas from the Chalmers biomass gasifier. The experiment showed that the catalyst was continuously regenerated from carbon deposits, and the ilmenite reduced the total amount of tar by 35 % at a gas residence time in the bed of 0.4–0.5 s. The tar cleaning process explored in this work is based on the CLR process, originally presented by Mattisson et al. [128]. The basic mechanism is to provide less oxygen for the reactions that take place in the fuel reactor.. The air reactor is used as a catalyst regeneration reactor, whereas in the fuel reactor, referred as reformer, the gas is fed with important tar concentrations. In this case, the proposed system which is shown in Fig. 20, has to be connected to a gasifier which provides the rich-tar gas.

3.4. Chemical looping gasification

Chemical Looping Gasification (CLG) is a promising technology that uses lattice oxygen instead of expensive gaseous oxygen for high quality syngas production without CO$_2$ emissions. Condori et al. [51] studied for the first time the behaviour of ilmenite as oxygen carrier in a 1.5 kW$_{th}$ CLG continuous unit to obtain a highly concentrated synthesis gas stream using pine wood as fuel during 55 h of operation. The high biomass conversions, higher than 90 %, and carbon conversion efficiencies, about 90 %, demonstrated the high CO$_2$ capture inherent to the CLG processes. It is noteworthy the low tar contents generated, below 3 g/kg dry biomass (<2 g/Nm^3 d.b.), which represents a clear advantage of CLG with respect to other syngas production processes. The characterization of ilmenite after CLG operation showed a reduction of lifetime with respect to CLC conditions mainly due to the highly reduced state of the oxygen carrier in the fuel reactor. Regardless, ilmenite can be considered as a suitable oxygen carrier to be used in CLG processes for high quality syngas production without CO$_2$ emissions to the atmosphere. Another recent work of Chalmers university investigated the use of ilmenite for the gasification of biomass in a 300 W chemical looping unit [129]. Two oxygen carriers were compared: ilmenite and LD slag. The working temperature was between 850 °C and 900 °C. The main results of this work were the following: 1) the Norwegian ilmenite had generally a higher reactivity compared to LD slag and this was independent of temperature and fuel flow; 2) ilmenite had better performance in terms of methane conversion than LD slag; 3) ilmenite exhibited higher resistance to attrition than LD slag. Based on these results it could be concluded that ilmenite was a preferable oxygen carrier for CLG processes compared to LD slag.

4. Design, modeling and validation of CLC

Design, modeling and validation of experimental data of existing CLC pilot plants is a key aspect in order to move forward with the development and scaling up to industrial CLC plants. Currently there are some
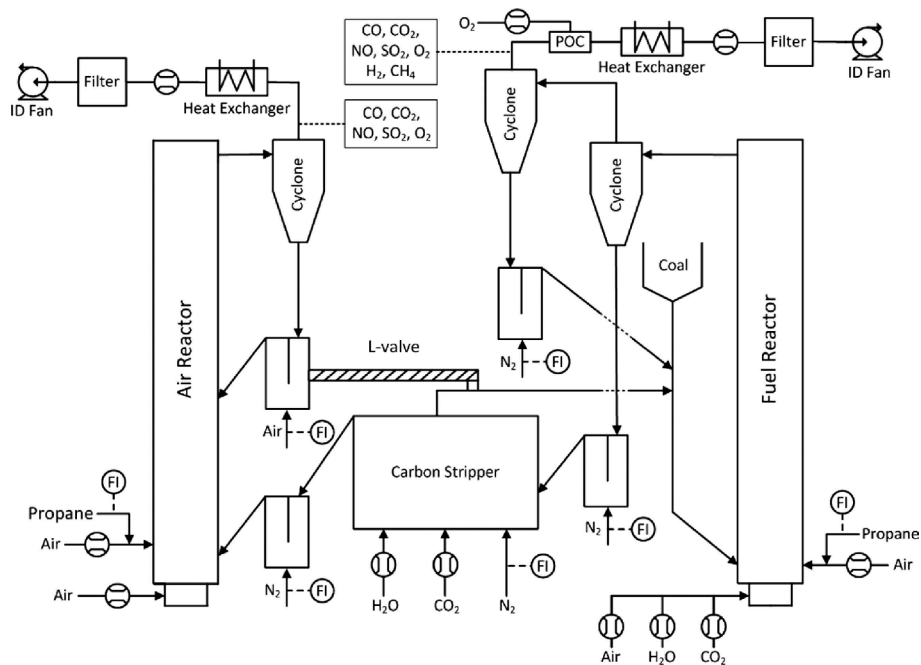
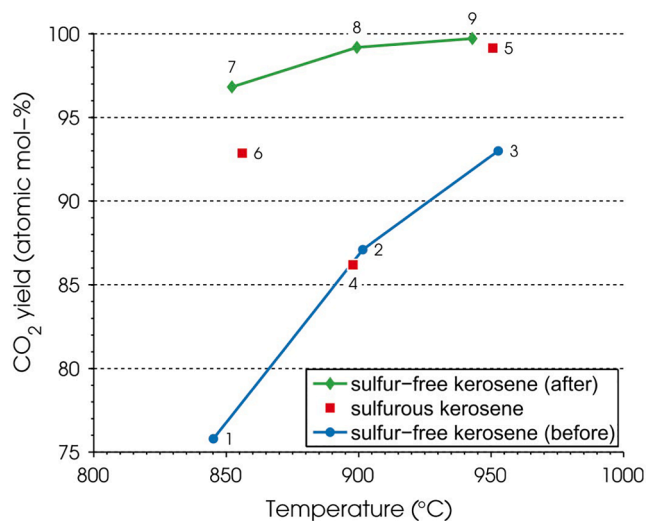**Fig. 17.** 1 MW$_{th}$ unit for solid fuels at Darmstadt university [106].

Fig. 18. Carbon dioxide yields with different types of kerosene [109].

CLC research works related to pilot plants ranging from 50 kW$_{th}$ to 1 MW$_{th}$, which use ilmenite as oxygen carrier.

Abad et al. [102] developed the design and the simulation model of a 50 kW$_{th}$ CLC located at ICB-CSIC, Spain, that could operate in either iG-CLC or CLOU mode. The pilot plant consists of a fuel reactor, an air reactor and a carbon stripper. In order to control independently the solid circulation rate from solids inventory of the fuel reactor, a double loop seal was installed. Fig. 21 shows a general scheme of the installation. Ilmenite was selected as bed material. Satisfactory results were obtained during the experimental campaign in iG-CLC mode operating at temperatures between 900 and 990 °C. High CO$_2$ capture efficiencies with low oxygen demand (7.5 %) were reached. It was observed that the char conversion was highly dependent on the fuel reactor temperature, increasing from 51 % at 900 °C to 84.7 % at 990 °C. Therefore, the higher temperature the higher CO$_2$ capture. Additionally, the fuel reactor temperature hardly affected the oxygen demand.

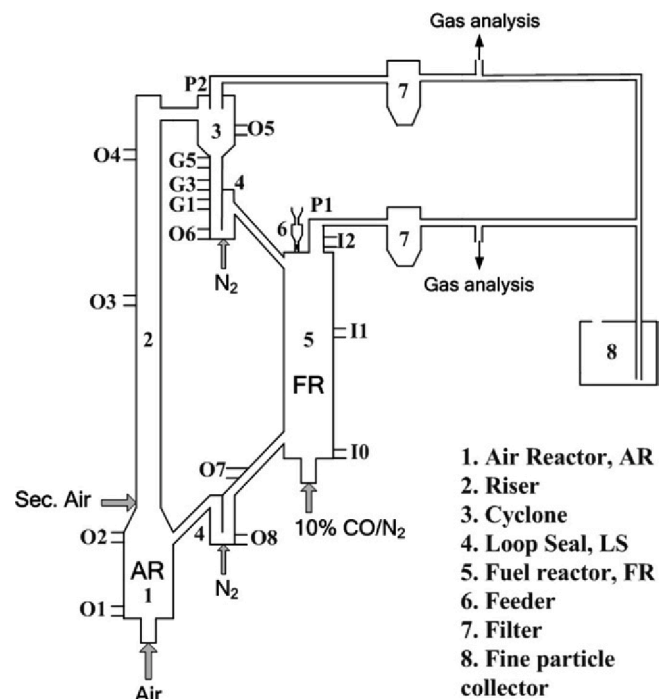Abad et al. [130] developed a 1.5D model based on semi-empirical

Fig. 19. Dual fluidized bed configuration developed at Tsinghua University [115].

correlations that was capable of describing the performance of the fuel reactor of 1 MW$_{th}$ coal-fired CLC plant using ilmenite as bed material, which is located in Technology University of Darmstadt. The pilot plant is equipped at the exit of the fuel reactor with two cyclones, low and high efficiency, to recover the elutriated oxygen carrier particles and a carbon stripper to improve the carbon separation before the oxygen carrier particles return to the air reactor, see Fig. 22.

The proposed model provided interesting results about reactor fluid-dynamics, product gas concentrations along the reactor, axial oxygen carrier conversion, axial carbon conversion, and char flow to the air

reactor. The reactor fluid-dynamics was developed based on a previous work performed by Pallares and Johnsson [131] in which the fuel reactor is divided into two regions, the bottom bed and the freeboard. The bottom bed was characterized by presenting a high and roughly constant solids concentration with a gas exchange between bubbles and emulsion which is at minimum fluidization velocity so that the excess of flow over the minimum gas velocity, u_{mf}, was distributed between the visible gas in the rising bubbles, u_{vis}, and the throughflow, u_{tf}. The freeboard, which is just above the bottom bed was characterized by presenting a splash or cluster phase and a transport or dispersed phase with an abrupt decay in solids concentration and a core/annulus structure, see Fig. 22. The operating conditions of the simulated reference case are shown in Table 8. The solids hold-up in the 1 MW$_{th}$ CLC plant was 260 kg operating at high velocity regime with a residence time of oxygen carrier particles of 100 s.

They observed that under reference conditions, the carbon capture value with a carbon separation efficiency of 90 % was low (59 %) with a relatively high oxygen demand (10.5 %). Nevertheless, the carbon capture efficiency increased to 95 % if the carbon separation efficiency was as high as 99 %. Therefore, the carbon separation played an important role in the process.

Garcia-Labiano et al. [132] also carried out further simulation and optimization study for the same 1 MW$_{th}$ coal-fired CLC with ilmenite as oxygen carrier. The authors conducted a sensitivity analysis analyzing the effect of the main operating variables - the efficiency of the carbon separation system, the solids inventory in the fuel reactor, the temperature in the fuel reactor, ratio of oxygen carrier to fuel, oxygen carrier reactivity, coal reactivity and coal particle - on the carbon capture and combustion efficiency of the process. This analysis revealed that the char

residence time and the temperature were the most important factors affecting the char conversion. They also stated that it was possible to attain high carbon capture efficiency (98.6 %) and a relatively low oxygen demand (6.8 %) as long as the temperature in the fuel reactor was 1100 °C and the solids inventory and the efficiency of the carbon separation system were 1000 kg/MW$_{th}$ and 98 %, respectively.

In other research work, Abad et al. [97] conducted the validation of the mathematical model described above with experimental data from a 100 kW$_{th}$ CLC pilot plant using ilmenite as bed material located in Chalmers University of Technology, Sweden. The validation of a model is a key factor and a very useful tool for the design of the fuel reactor and also for the optimization the CLC process. Satisfactory concordance between experimental and theoretical data were obtained. It was found that the oxygen demand was highly dependent on the reactor temperature, the solids circulation flow rate and the solids inventory. Moreover, a CO$_2$ capture efficiency of η_{CC} = 98.5 % and a total oxygen demand of Ω_T = 9.6 % was determined, operating at 1000 °C and with a solid inventory of 1500 kg/MW$_{th}$ in the fuel reactor. Then, the validated model was used to design a 50 kW$_{th}$ iG-CLC unit. Experimental results achieved during the operation of this facility were in agreement with information provided by the developed model.

Similarly a model on 1D process of 1 MW$_{th}$ CLC plant was developed in the work of [133]. Gayán et al. [134] performed an extensive assessment of different technical option to improve the combustion efficiency in iG-CLC systems. They suggested five different alternatives based on 1) equipping the reactor with internal in order to enhance the gas–solid mixing; 2) installing a secondary fuel reactor for the unburnt gas products from main fuel reactor; 3) recycling of unburnt product gases to either fuel reactor or carbon stripper; 4) separation and
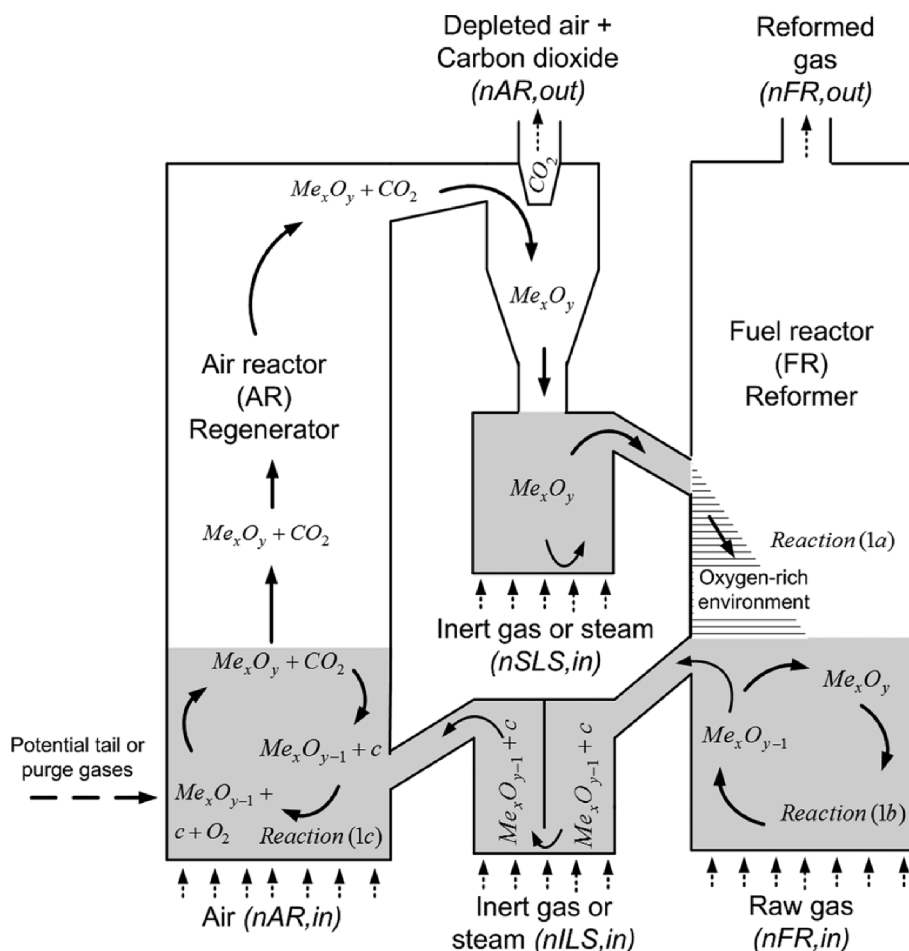

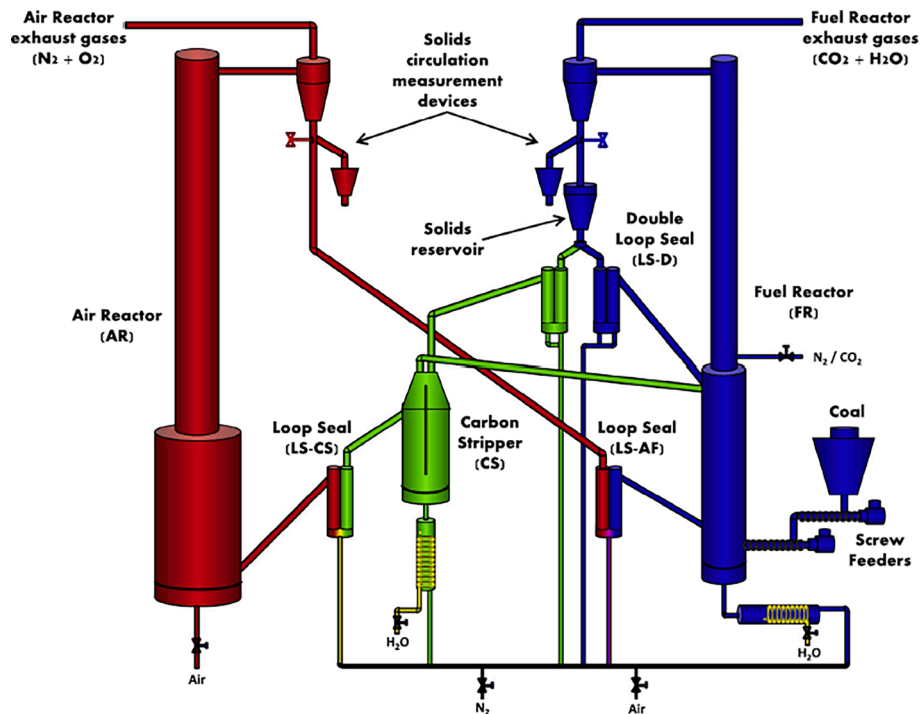**Fig. 20.** Chemical Looping Reforming for upgrading of biomass producer gas [124].

Fig. 21. Schematic of the 50kW$_{th}$ CLC pilot plant located at ICB-CSIC [102].

recycling of unburnt product gases to the fuel reactor; and 5) supplying coal to the carbon stripper so that the fuel reactor turns into a secondary fuel reactor, see Fig. 23.

The simulation results showed that the implementation of a

secondary fuel reactor was the best alternative to achieve the lowest oxygen demand values. So, the proposed configuration lain in using the carbon stripper as a secondary fuel reactor, as it is shown in Fig. 24.

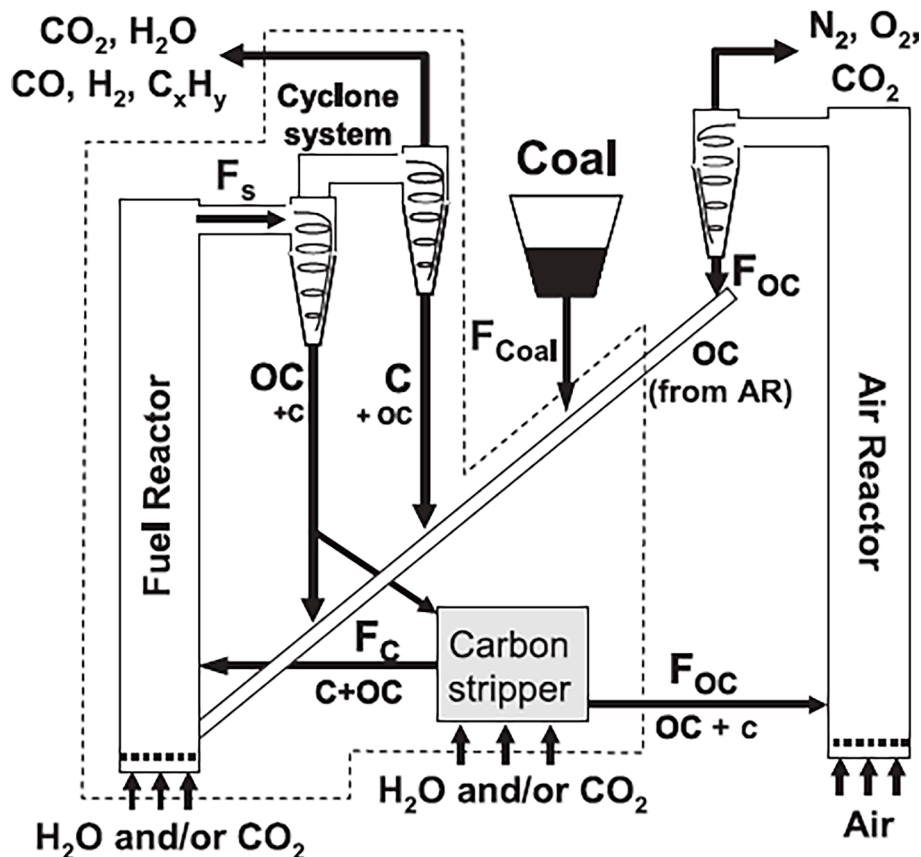A conceptual design and model of a 100 MW$_{th}$ coal-fired iG-CLC

Fig. 22. Schematic of the 1MW$_{th}$ CLC pilot plant located at TU Darmstadt [130].

Table 8
Main operating conditions for the reference case studied [130].

Operating conditions	Symbol	Value	Units
Temperature	T	1,000	°C
Pressure at the outlet	P	101,325	Pa
Pressure drop	ΔP_0	20,000	Pa
Inlet gas flow (steam)	$Q_{g,in}$	77	Nm^3/h^{-1}
Gas flow from carbon stripper (CS) (steam)	$Q_{g,cs}$	213	Nm^3 h^{-1}
Efficiency of the CCS	η_{CSS}	0.9	–
Rate of coal feeding	F_{coal}	140	kg h^{-1}
Solids circulation rate	F_{OC}	9,300	kg h^{-1}
Oxygen carrier-to-fuel ratio	Φ	1.2	–
Solids conversion at the fuel reactor inlet	$\overline{X}_{OC,in}$	0	–

plant using ilmenite as oxygen carrier was outlined by Abad et al. [135], see Fig. 25.

Mass and heat balances together with the fluid-dynamic [131] and cyclones sizing were considered. It was observed that cyclones sizing strongly affected the measurements of the three main components: fuel and air reactor, and carbon stripper. A solids inventory of 750 kg/MW$_{th}$ in the fuel reactor was predicted. Likewise, it was detected that the use

of CO$_2$, instead of steam, for fluidization improved the CO$_2$ capture and the oxygen demand need. CO$_2$ capture of 95 % with an oxygen demand of 7 % were obtained.

Another conceptual study of a 1000 MW$_{th}$ CLC power plant was suggested by Lyngfelt et al. [136] using ilmenite as oxygen carrier. It took into account both mass and heat balances, solids inventory and fuel and air reactor sizing. In this design, no carbon stripper was considered since, at large scale, it is expected that the height of the fuel reactor be sufficiently high (5 m) as to operate itself as carbon stripper.

There are also some research works focused on computational fluid dynamic (CFD) models with ilmenite. Sandu et al. [137] developed a simulation in COMSOL Multiphysics of the mass and energy balances together with the momentum balance of a single particle in a packed bed. The CFD particle model was coupled with a 0D model describing the macroscale interactions in the packed bed. The 0D model was validated with the breakthrough curves measured by Gallucci et al.[138]. The results of the particle model produced a detailed description of the temperature field in the particle, see Fig. 26, and a description of the concentration of Fe$_2$O$_3$ and FeO during the reduction process, see Fig. 27.
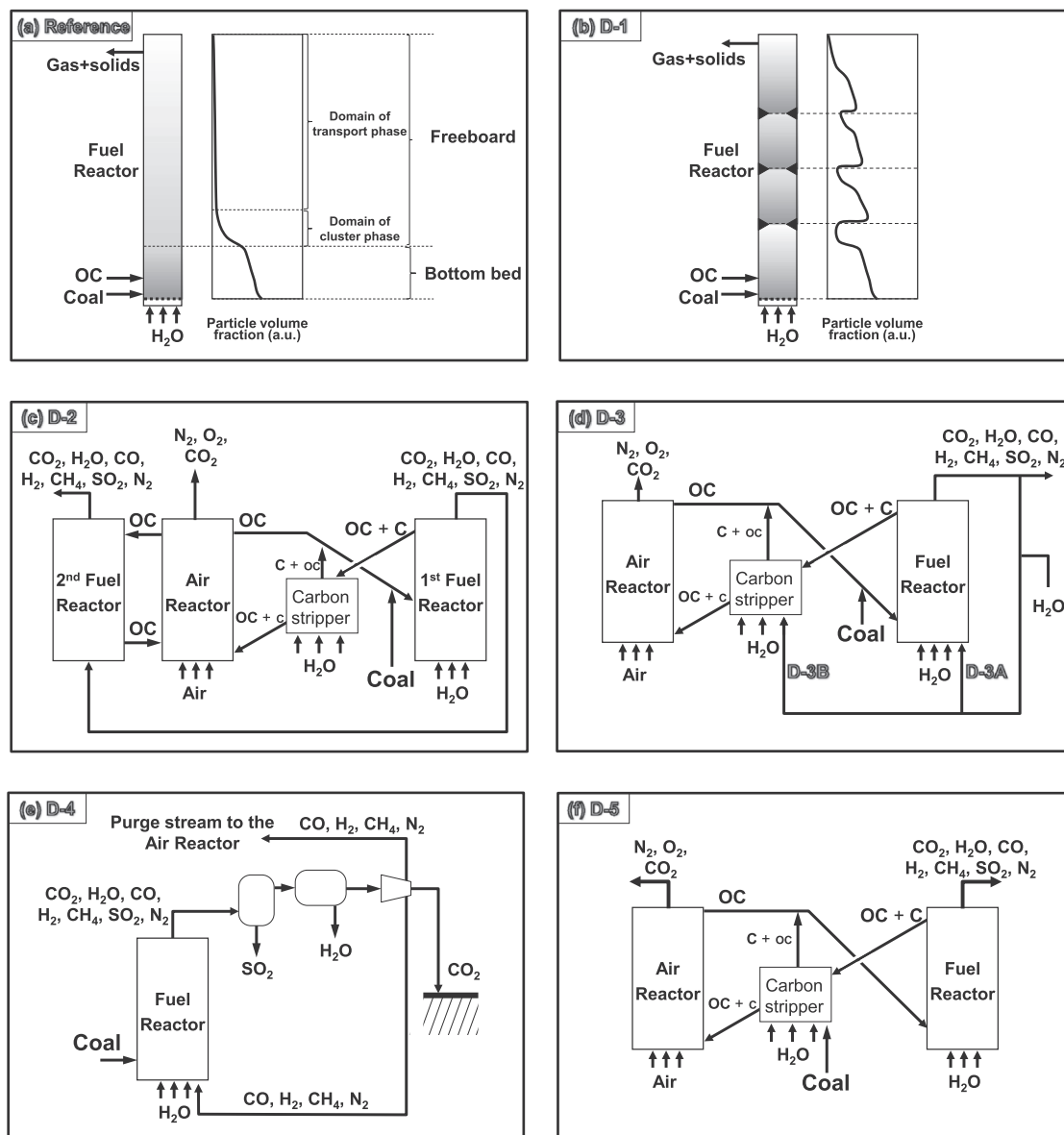

Fig. 23. Different options considered in the study of Gayán et al. [134].
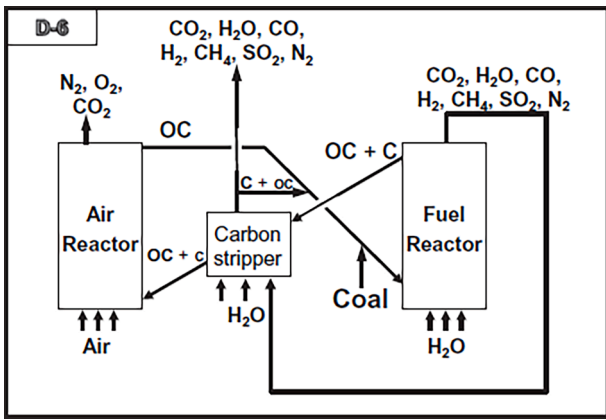
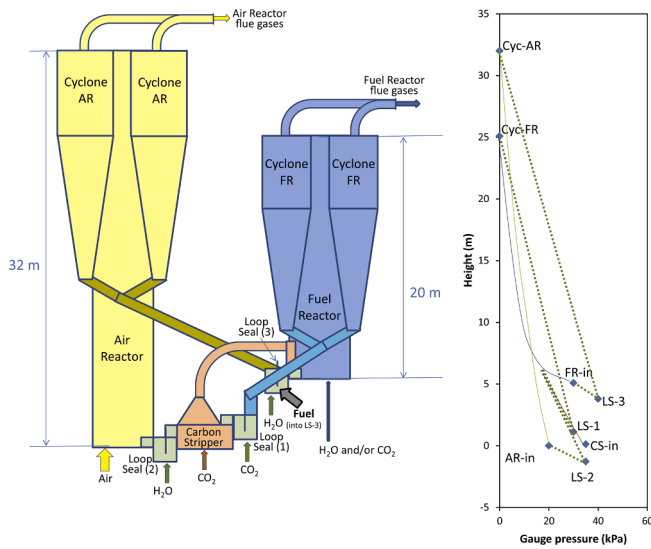**Fig. 24.** Scheme of the new proposed iG-CLC configuration [134].

Fig. 25. Conceptual design and model of a 100 MW$_{th}$ coal-fired iG-CLC and pressure profile, according to [135].

Fig. 26. Change in temperature in the 3D particle model at 30 s [138].

5. Technical and economic analysis

A key aspect required to scale-up chemical looping technologies towards commercial deployment is having detailed and verified techno-economic analyses allowing for a reliable evaluation of whether these technologies are technically feasible, competitive in terms of energy efficiency and profitable from an economic point-of-view. In the particular case of ilmenite, there are very few techno-economic studies carried out to date that compare the potential of chemical looping technologies using this material as an oxygen carrier with that related to other energy processes with and without integration of CO$_2$ capture technologies.

Regarding the use of ilmenite in chemical looping processes with gaseous fuels, Symonds et al. [139] carried out a study of the potential for replacement once-through steam generators (OTSGs) at steam assisted gravity drainage (SAGD) facilities for the production of bitumen by using PCLC technology with natural gas as fuel. In this work, it was determined that the optimum operating pressure range in the PCLC unit was between 4 and 7 bar (g) to maximize power generation. The replacement of the OTSG units by PCLC technology also brought about a reduction in the consumption of natural gas and boiler feed water (BFW) make-up of 8 and 38.4 %, respectively, as well as a drop in CO$_2$ emissions of 95 %. This work was completed with an economic analysis of
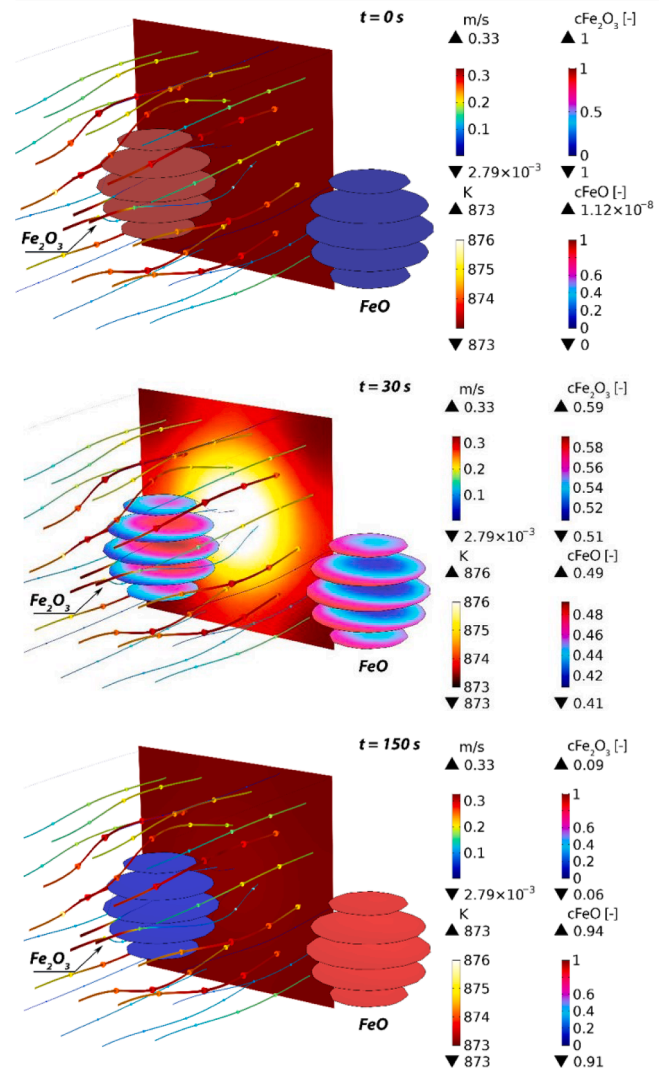

Fig. 27. Change in oxygen carrier composition at 0 s (in the top), 30 s (in the middle), and 150 s (in the bottom).
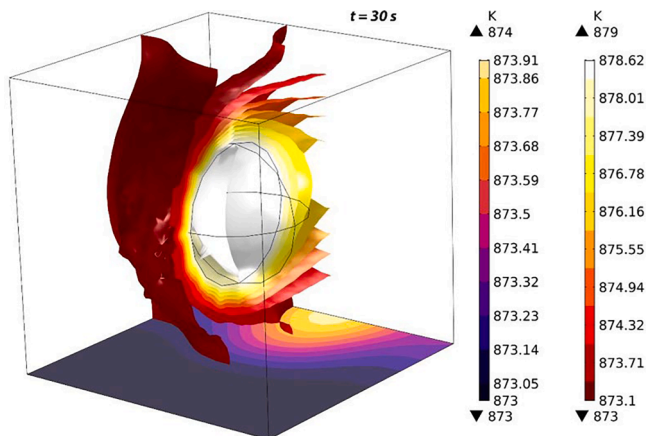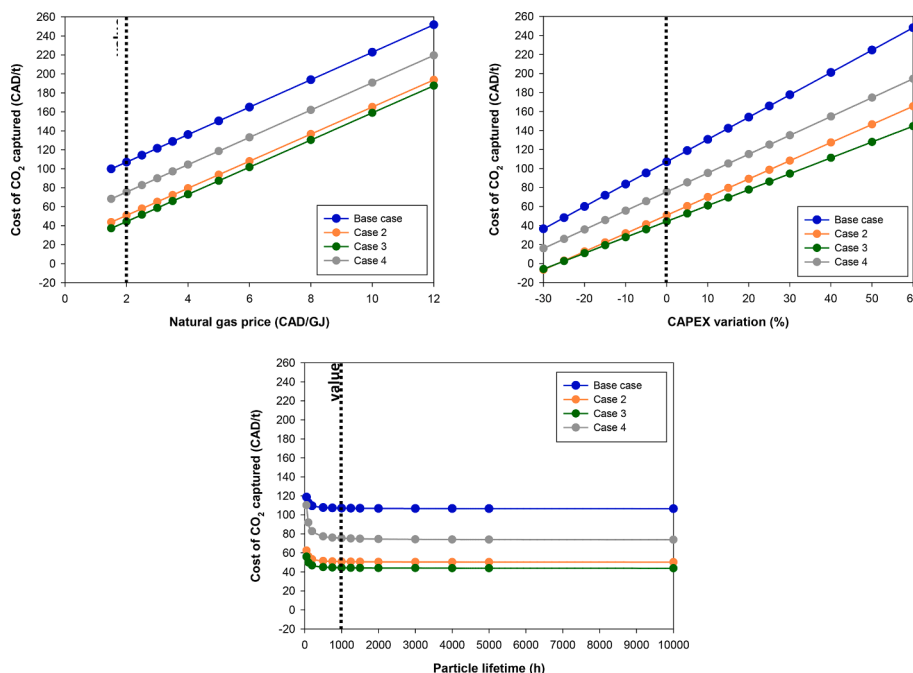
Fig. 28. Effect of natural gas price, CAPEX variation and particle lifetime on the cost of CO_2 captured. Adapted from Ref. [140].

four different configurations of the PCLC-SAGD process, three at a pressure of 7 bar (g) and one at atmospheric pressure [140]. The main profitability parameter evaluated was the Levelized Cost of Steam (LCOS), which took a value between 30.45 and 39.93 CAD/t. The cost of CO_2 captured was also calculated, which ranged between 44.39 and 107.05 CAD/t of CO_2. All of these values were considerably lower compared to those found in the literature using other CCS technologies for the same industrial process. A thorough sensitivity analysis of the main factors that may affect the economic result of the project was also carried out, and it was found that whereas the cost of natural gas and CAPEX had a very important influence on the economic profitability, the cost and the particle lifetime of ilmenite ore particles had a negligible effect, see Fig. 28. In this work, the sensitivity analysis of the oxygen carrier cost was not carried out, but understanding this parameter is critical for the successful development of an economic chemical looping combustion process. To date, oxygen carrier costs have been estimated from small-scale tests and production, grounded at best by vendor quotes from toll manufacturers at "ton" quantities of material. Commercial-scale CLC operations will require oxygen carrier inventories on the order of thousands of tons. In this regard, National Energy Technology Laboratory (NETL) carried out a study to estimate the cost as a function of production volume for different to-be-determined oxygen carrier material classes [141]. This thorough study includes nine relevant tasks: oxygen carrier specifications, preparation procedures, production facility scenarios, oxygen carrier production rate range, raw material sources and prices, production facility descriptions, material & energy balances, production facility capital cost, and oxygen carrier makeup cost. In the particular case of ilmenite, the study concluded that the price for a manufacturing plant that produces 1340 kg/h of material was between 0.42 and 0.64 USD/kg, values well below the cost target of 5 USD/kg established by NETL [141].

Zhu et al. [142] carried out a techno-economic analysis of a 200 MW$_{th}$ CLC plant for power production from natural gas using three oxygen carriers based on nickel oxide, copper oxide and ilmenite, respectively. The results with ilmenite were very satisfactory since a maximum net power efficiency of 48.02 % and a Levelized Cost of Electricity (LCOE) of 71.98 €/MWh were obtained, only € 0.32/MWh higher than that achieved for the most profitable case, i.e., the nickel-based case. Furthermore, in all cases, the specific CO_2 emissions were

much lower than those that would be obtained in a Natural Gas Combined Cycle (NGCC) power plant with CO_2 capture.

As previously mentioned, ilmenite ore has been used especially in CLC processes for the conversion of solid fuels, mainly coal. In this regard, Lyngfelt and Leckner [136] have carried out the most ambitious techno-economic analysis to date on the scaling-up of CLC technology for solid fuels, up to the 1000 MW$_{th}$ range, establishing the main differences between a full-scale Circulating Fluidized-Bed (CFB) boiler and a Chemical-Looping Combustion CFB (CLC – CFB) and considering the use of ilmenite as oxygen carrier. From an economical point of view, it was concluded that the additional cost of CLC-CFB relative to CFB technology was around 20 €/t CO_2. Of this amount, between 4 and 9 €/t CO_2 corresponded to the oxygen polishing stage and between 1.3 and 4 €/t CO_2 were attributed to the cost of the oxygen carrier assuming a very conservative value of particle lifetime of 100–300 h. Finally, Tsupari et al. [143] analyzed the techno-economic feasibility of a 482 MW$_{th}$ commercial-scale CLC power plant located on the coast of the Gulf of Bothnia, Finland, using coal as fuel and ilmenite as oxygen carrier. In this study, the CLC plant was compared with a reference case plant, an air-fired CFB plant without CCS, and an oxy-fired CFB plant. These authors found that the production of electricity through CLC could become more competitive compared to other CCS technologies if the CO_2 market set a relatively high price since CLC technology achieved higher electrical efficiencies. Specifically, for the Finnish electricity market scenario and considering a CO_2 allowances of 50 €/t CO_2, the electricity production cost for CLC was between 40 and 45 €/MWh, whereas this value increased up to 50 and 65 €/MWh for the oxy-fuel case and reference case without CCS, respectively.

6. Conclusions

This work is a comprehensive review of the properties, use and performance of ilmenite as oxygen carrier for chemical looping and oxygen carrier aided combustion technologies. In particular, the paper gathers information regarding physic–chemical properties of ilmenite and highlights the changes in terms of composition, reactivity, iron migration, and species segregation underwent by the particles during calcination and oxidation stages. Furthermore, the reduction and oxidation kinetics are compiled at both atmospheric and pressurized

conditions. Likewise, this work describes the most relevant aspects related to the thermodynamics of ilmenite as well as mass and energy balances for chemical looping processes. The performance of ilmenite for CLC, CLR, CLG, and OCAC systems with different types of fuels has been thoroughly revised providing the most important results obtained up to date. Finally, the main techno-economic analyses involving the use of ilmenite as oxygen carrier have been summarized in order to get an insight into the effect of this material on the profitability of chemical looping facilities.

CRediT authorship contribution statement

Pietro Bartocci: Conceptualization, Methodology, Validation, Formal analysis, Investigation, Writing – original draft, Writing – review & editing, Visualization, Funding acquisition. **Alberto Abad:** Conceptualization, Methodology, Validation, Resources, Investigation, Data curation, Visualization, Supervision, Funding acquisition. **Arturo Cabello Flores:** Conceptualization, Methodology, Validation, Formal analysis, Investigation, Writing – original draft, Writing – review & editing, Visualization. **Margarita de las Obras Loscertales:** Conceptualization, Methodology, Validation, Resources, Visualization, Writing – original draft, Writing – review & editing.

Declaration of Competing Interest

The authors declare that they have no known competing financial interests or personal relationships that could have appeared to influence the work reported in this paper.

Data availability

Data will be made available on request.

Acknowledgments

References

[1] Mendiara T, et al. Negative CO2 emissions through the use of biofuels in chemical looping technology: a review. Appl Energy 2018;232:657–84.
[2] Mendiara T, et al. Process comparison for biomass combustion: in situ gasification-chemical looping combustion (iG-CLC) versus chemical looping with oxygen uncoupling (CLOU). Energ Technol 2016;4(10):1130–6.
[3] Abanades J, et al. Emerging CO2 capture systems. Int J Greenhouse Gas Control 2015;40:126–66.
[4] Leion H, et al. The use of ilmenite as an oxygen carrier in chemical-looping combustion. Chem Eng Res Des 2008;86(9):1017–26.
[5] Rydén M, et al. Oxygen carrier aided combustion (OCAC) of wood chips in a semi-commercial circulating fluidized bed boiler using manganese ore as bed material. Appl Sci 2016;6(11):347.
[6] Leion H, Mattisson T, Lyngfelt A. Use of ores and industrial products as oxygen carriers in chemical-looping combustion. Energy Fuel 2009;23(4):2307–15.
[7] Lyngfelt A. Oxygen carriers for chemical looping combustion-4 000 h of operational experience. Oil & Gas Science and Technology-Revue d'IFP Energies nouvelles 2011;66(2):161–72.
[8] Adanez J, et al. Progress in chemical-looping combustion and reforming technologies. Prog Energy Combust Sci 2012;38(2):215–82.
[9] Zeng L, et al. Chemical looping processes—particle characterization, ionic diffusion-reaction mechanism and reactor engineering. Rev Chem Eng 2012;28 (1):1–42.
[10] Larring Y, et al. Fe–Mn based minerals with remarkable redox characteristics for chemical looping combustion. Fuel 2015;159:169–78.
[11] Luo S, Zeng L, Fan L-S. Chemical looping technology: oxygen carrier characteristics. Annu Rev Chem Biomol Eng 2015;6:53–75.

[12] Wang P, et al. Chemical-looping combustion and gasification of coals and oxygen carrier development: a brief review. Energies 2015;8(10):10605–35.
[13] Nandy A, et al. Present status and overview of Chemical Looping Combustion technology. Renew Sustain Energy Rev 2016;59:597–619.
[14] Batra VS, Li H-P. Oxygen carrier materials and their role in chemical looping reactions for fuel conversion. Curr Opin Chem Eng 2017;15:44–8.
[15] Gauthier T, et al. CLC, a promising concept with challenging development issues. Powder Technol 2017;316:3–17.
[16] Li J, et al. CO2 capture with chemical looping combustion of gaseous fuels: an overview. Energy Fuel 2017;31(4):3475–524.
[17] Matzen M, et al. Use of natural ores as oxygen carriers in chemical looping combustion: a review. Int J Greenhouse Gas Control 2017;65:1–14.
[18] Adánez J, et al. Chemical looping combustion of solid fuels. Prog Energy Combust Sci 2018;65:6–66.
[19] Cheng Z, et al. New insight into the development of oxygen carrier materials for chemical looping systems. Engineering 2018;4(3):343–51.
[20] Mattisson T, et al. Chemical-looping technologies using circulating fluidized bed systems: status of development. Fuel Process Technol 2018;172:1–12.
[21] Adánez J, Abad A, Chemical-looping combustion: Status and research needs. Proceedings of the Combustion Institute, 2019. 37(4): p. 4303-4317.
[22] Yu Z, et al. Iron-based oxygen carriers in chemical looping conversions: a review. Carbon Resources Conversion 2019;2(1):23–34.
[23] Lyngfelt A, et al. 11,000 h of chemical-looping combustion operation—where are we and where do we want to go? Int J Greenhouse Gas Control 2019;88:38–56.
[24] De Vos Y, et al. Development of Stable oxygen carrier materials for chemical looping processes—a review. Catalysts 2020;10(8):926.
[25] Lyngfelt A. Chemical looping combustion: status and development challenges. Energy Fuel 2020;34(8):9077–93.
[26] Li D, et al. Chemical-looping conversion of methane: a review. Energ Technol 2020;8(8):1900925.
[27] Yu L, et al. Developing oxygen carriers for chemical looping biomass processing: challenges and opportunities. Advanced Sustainable Systems 2020;4(12): 2000099.
[28] Osman M, et al. Review of pressurized chemical looping processes for power generation and chemical production with integrated CO2 capture. Fuel Process Technol 2021;214:106684.
[29] Qasim M, et al. Recent advances and development of various oxygen carriers for the chemical looping combustion process: a review. Ind Eng Chem Res 2021.
[30] Berguerand N, Lyngfelt A. Chemical-looping combustion of petroleum coke using ilmenite in a 10 kWth unit– high-temperature operation. Energy Fuel 2009;23 (10):5257–68.
[31] Azis MM, et al. On the evaluation of synthetic and natural ilmenite using syngas as fuel in chemical-looping combustion (CLC). Chem Eng Res Des 2010;88(11): 1505–14.
[32] Rydén M, et al. Ilmenite with addition of NiO as oxygen carrier for chemical-looping combustion. Fuel 2010;89(11):3523–33.
[33] Berguerand N, Lyngfelt A. Batch testing of solid fuels with ilmenite in a 10 kWth chemical-looping combustor. Fuel 2010;89(8):1749–62.
[34] Sanchez-Segado S, Lahiri A, Jha A. Alkali roasting of bomar ilmenite: rare earths recovery and physico-chemical changes. Open Chemistry 2015;13(1).
[35] Parirenyatwa S, et al. Comparative study of alkali roasting and leaching of chromite ores and titaniferous minerals. Hydrometall 2016;165:213–26.
[36] Symonds RT, et al. Ilmenite ore as an oxygen carrier for pressurized chemical looping reforming: Characterization and process simulation. Int J Greenhouse Gas Control 2019;81:240–58.
[37] Sun Z, et al. Enhanced performance of ilmenite modified by CeO2, ZrO2, NiO, and Mn2O3 as oxygen carriers in chemical looping combustion. Appl Energy 2017; 195:303–15.
[38] Campos DC, Belkouch J, Hazi M, Reactivity investigation on iron-titanium oxides for a moving bed chemical looping combustion implementation. 2013.
[39] Yamaguchi D, Tang L, Chiang K. Pre-oxidation of natural ilmenite for use as an oxygen carrier in the cyclic methane–steam redox process for hydrogen production. Chem Eng J 2017;322:632–45.
[40] Adánez J, et al. Ilmenite activation during consecutive redox cycles in chemical-looping combustion. Energy Fuel 2010;24(2):1402–13.
[41] Bhogeswara Rao D, Rigaud M. Kinetics of the oxidation of ilmenite. Oxid Met 1975;9(1):99–116.
[42] Ridha FN, et al. Characterization of an ilmenite ore for pressurized chemical looping combustion. Appl Energy 2016;163:323–33.
[43] Cuadrat A, et al. Behavior of ilmenite as oxygen carrier in chemical-looping combustion. Fuel Process Technol 2012;94(1):101–12.
[44] Miya K, Otomo J. Improvements in reaction kinetics and stability of ilmenite as oxygen carrier by surface modification with calcium titanate in redox cycles of chemical-looping systems. Chem Eng J 2017;327:257–67.
[45] Qin L, et al. Nanostructure formation mechanism and ion diffusion in iron–titanium composite materials with chemical looping redox reactions. J Mater Chem A 2015;3(21):11302–12.
[46] Li F, et al. Ionic diffusion in the oxidation of iron—effect of support and its implications to chemical looping applications. Energ Environ Sci 2011;4(3): 876–80.
[47] Liu Y-C, et al. Reduction mechanism of iron titanium based oxygen carriers with H 2 for chemical looping applications–a combined experimental and theoretical study. RSC Adv 2016;6(108):106340–6.
[48] Feng Y, et al. Characteristics of dopant distribution and surface oxygen vacancy formation for modified Fe2O3 in chemical looping combustion. Fuel 2020;276: 117942.

[49] Huang L, et al. Density functional theory study on the reaction between hematite and methane during chemical looping process. Appl Energy 2015;159:132–44.

[50] Cheng Z, et al. Methane adsorption and dissociation on iron oxide oxygen carriers: the role of oxygen vacancies. PCCP 2016;18(24):16423–35.

[51] Condori O, et al. Biomass chemical looping gasification for syngas production using ilmenite as oxygen carrier in a 1.5 kWth unit. Chem Eng J 2021;405:126679.

[52] Jamanca-Lino G. Space resources engineering: ilmenite deposits for oxygen production on the moon. Am J Min Metall 2021;6:6–11.

[53] Rydén M, et al. Release of gas-phase O2 from ilmenite during chemical-looping combustion experiments. Chem Eng Technol 2012;35(11):1968–72.

[54] Abad A, et al. Mapping of the range of operational conditions for Cu-, Fe-, and Ni-based oxygen carriers in chemical-looping combustion. Chem Eng Sci 2007;62(1–2):533–49.

[55] Hallberg P, Leion H, Lyngfelt A. A method for determination of reaction enthalpy of oxygen carriers for chemical looping combustion–application to ilmenite. Thermochim Acta 2011;524(1–2):62–7.

[56] Azis MM, et al. The effect of bituminous and lignite ash on the performance of ilmenite as oxygen carrier in chemical-looping combustion. Chem Eng Technol 2013;36(9):1460–8.

[57] Abad A, et al. Kinetics of redox reactions of ilmenite for chemical-looping combustion. Chem Eng Sci 2011;66(4):689–702.

[58] Cuadrat A, et al. The use of ilmenite as oxygen-carrier in a 500 Wth Chemical-Looping Coal Combustion unit. Int J Greenhouse Gas Control 2011;5(6):1630–42.

[59] Johansson M, Mattisson T, Lyngfelt A. Investigation of Fe2O3 with MgAl2O4 for chemical-looping combustion. Ind Eng Chem Res 2004;43(22):6978–87.

[60] Cuadrat A, et al. Prompt considerations on the design of chemical-looping combustion of coal from experimental tests. Fuel 2012;97:219–32.

[61] Cuadrat A, et al. Effect of operating conditions in Chemical-Looping Combustion of coal in a 500 Wth unit. Int J Greenhouse Gas Control 2012;6:153–63.

[62] Cuadrat A, et al. Relevance of the coal rank on the performance of the in situ gasification chemical-looping combustion. Chem Eng J 2012;195:91–102.

[63] Johansson M, Mattisson T, Lyngfelt A. Comparison of oxygen carriers for chemical-looping combustion. Therm Sci 2006;10(3):93–107.

[64] Zerobin F, et al. Fluidized bed reactor design study for pressurized chemical looping combustion of natural gas. Powder Technol 2017;316:569–77.

[65] Garcia-Labiano F, et al. Effect of pressure on the behavior of copper-, iron-, and nickel-based oxygen carriers for chemical-looping combustion. Energy Fuel 2006;20(1):26–33.

[66] Lee D, et al. Experimental screening of oxygen carrier for a pressurized chemical looping combustion. Fuel Process Technol 2021;218:106860.

[67] Tan Y, et al. Reduction kinetics of ilmenite ore as an oxygen carrier for pressurized chemical looping combustion of methane. Energy Fuel 2017;31(7):7598–605.

[68] Tan Y, et al. Effects of H2S on the reactivity of ilmenite ore as chemical looping combustion oxygen carrier with methane as fuel. Energy Fuel 2018;33(1):585–94.

[69] Lu X, et al. Pressurized chemical looping combustion with CO: Reduction reactivity and oxygen-transport capacity of ilmenite ore. Appl Energy 2016;184:132–9.

[70] Zaabout A, Cloete S, Amini S. Autothermal operation of a pressurized Gas Switching Combustion with ilmenite ore. Int J Greenhouse Gas Control 2017;63:175–83.

[71] Rana S, et al. Ilmenite oxidation kinetics for pressurized chemical looping combustion of natural gas. Appl Energy 2019;238:747–59.

[72] Thunman H, et al. Using an oxygen-carrier as bed material for combustion of biomass in a 12-MWth circulating fluidized-bed boiler. Fuel 2013;113:300–9.

[73] Lind F, Corcoran A, Thunman H. Validation of the oxygen buffering ability of bed materials used for OCAC in a large scale CFB boiler. Powder Technol 2017;316:462–8.

[74] Störner F, Lind F, Rydén M. Oxygen carrier aided combustion in fluidized bed boilers in Sweden—review and future outlook with respect to affordable bed materials. Appl Sci 2021;11(17):7935.

[75] Andersson B, et al. 4000 Hours of Operation with Oxygen-Carriers in Industrial Relevant Scale (75 MWth). 4th International conference on Chemical Looping. 2016.

[76] Zhao D, et al. Laboratory fluidized bed testing of ilmenite as bed material for oxygen carrier aided combustion (OCAC). in 11th International Conference on Fluidized Bed Technology, Beijing, China. 2014.

[77] Chadeesingh D, Hayhurst A. The combustion of a fuel-rich mixture of methane and air in a bubbling fluidised bed of silica sand at 700° C and also with particles of Fe2O3 or Fe present. Fuel 2014;127:169–77.

[78] Schneider T, et al. Investigation of the Oxygen Supply and Distribution in a Bubbling Fluidized Bed by Using Natural Ilmenite for Oxygen Carrier Aided Combustion. Energy Fuel 2021;35(15):12352–66.

[79] Garcia E, Liu H. Ilmenite as alternative bed material for the combustion of coal and biomass blends in a fluidised bed combustor to improve combustion performance and reduce agglomeration tendency. Energy 2021;121913.

[80] Moldenhauer P, et al. A scale-up project for operating a 115 MWth biomass-fired CFB boiler with oxygen carriers as bed material. Proceedings of the 5th International Conference on Chemical Looping. 2018.

[81] Hughes RW, Lu DY, Symonds RT. Improvement of oxy-FBC using oxygen carriers: concept and combustion performance. Energy Fuel 2017;31(9):10101–15.

[82] De Las Obras Loscertales M, L.D.Y., Li L, Hughes RW, Investigation of OCAC using canadian ilmenite ore in a circulating fluidized bed combustor. . CFB 2021 -

Proceedings of the 13th International Conference on Fluidized Bed Technology, Pages 509 – 5142021.

[83] Stenberg V, et al. Exploring novel hydrogen production processes by integration of steam methane reforming with chemical-looping combustion (CLC-SMR) and oxygen carrier aided combustion (OCAC-SMR). Int J Greenhouse Gas Control 2018;74:28–39.

[84] Corcoran A, et al. Comparing the structural development of sand and rock ilmenite during long-term exposure in a biomass fired 12 MWth CFB-boiler. Fuel Process Technol 2018;171:39–44.

[85] Corcoran A, et al. Industrial implementation of oxygen carrier aided combustion. 5th International Conference on Chemical Looping. 2018.

[86] Zevenhoven M, et al. Defluidization of the oxygen carrier ilmenite–Laboratory experiments with potassium salts. Energy 2018;148:930–40.

[87] Corcoran A, et al. Ash properties of ilmenite used as bed material for combustion of biomass in a circulating fluidized bed boiler. Energy Fuel 2014;28(12):7672–9.

[88] Staničić I, et al. Oxygen carrier aided combustion (OCAC) of two waste fuels-Experimental and theoretical study of the interaction between ilmenite and zinc, copper and lead. Biomass Bioenergy 2021;148:106060.

[89] Lind F, et al. 12,000 Hours of Operation with Oxygen-Carriers in Industrially Relevant Scale (75,000 kWth). VGB PowerTech 2017.

[90] Gyllén A, et al. Magnetic separation of ilmenite used as oxygen carrier during combustion of biomass and the effect of ash layer buildup on its activity and mechanical strength. Fuel 2020;269:117470.

[91] Berguerand N, Lyngfelt A. Design and operation of a 10 kWth chemical-looping combustor for solid fuels – testing with South African coal. Fuel 2008;87(12):2713–26.

[92] Berguerand N, Lyngfelt A. The use of petroleum coke as fuel in a 10 kWth chemical-looping combustor. Int J Greenhouse Gas Control 2008;2(2):169–79.

[93] Berguerand N, Lyngfelt A. Chemical-looping combustion of petroleum coke using ilmenite in a 10 kWth unit-high-temperature operation. Energy Fuel 2009;23(10):5257–68.

[94] Cuadrat A, et al. Influence of limestone addition in a 10 kWth chemical-looping combustion unit operated with petcoke. Energy Fuel 2011;25(10):4818–28.

[95] Linderholm C, et al. Chemical-looping combustion of solid fuels – operation in a 10 kW unit with two fuels, above-bed and in-bed fuel feed and two oxygen carriers, manganese ore and ilmenite. Fuel 2012;102:808–22.

[96] Markström P, Linderholm C, Lyngfelt A. Chemical-looping combustion of solid fuels – design and operation of a 100kW unit with bituminous coal. Int J Greenhouse Gas Control 2013;15:150–62.

[97] Abad A, et al. Fuel reactor model validation: assessment of the key parameters affecting the chemical-looping combustion of coal. Int J Greenhouse Gas Control 2013;19:541–51.

[98] Linderholm C, et al. Use of low-volatile solid fuels in a 100 kW chemical-looping combustor. Energy Fuel 2014;28(9):5942–52.

[99] Linderholm C, et al. Chemical-looping combustion in a 100-kW unit using a mixture of ilmenite and manganese ore as oxygen carrier. Fuel 2016;166:533–42.

[100] Cuadrat A, et al. The use of ilmenite as oxygen-carrier in a 500 Wth chemical-looping coal combustion unit. Int J Greenhouse Gas Control 2011;5:1630–42.

[101] Cuadrat A, et al. Relevance of the coal rank on the performance of the in situ gasification chemical-looping combustion. Chem Eng J 2012;195–196:91–102.

[102] Abad A, et al. Design and operation of a 50 kWth Chemical Looping Combustion (CLC) unit for solid fuels. Appl Energy 2015;157:295–303.

[103] Pérez-Vega R, et al. Coal combustion in a 50 kWth Chemical Looping Combustion unit: Seeking operating conditions to maximize CO2 capture and combustion efficiency. Int J Greenhouse Gas Control 2016;50:80–92.

[104] Thon A, et al. Operational experience with a system of coupled fluidized beds for chemical looping combustion of solid fuels using ilmenite as oxygen carrier. Appl Energy 2014;118:309–17.

[105] Ströhle J, Orth M, Epple B. Design and operation of a 1 MWth chemical looping plant. Appl Energy 2014;113:1490–5.

[106] Ströhle J, Orth M, Epple B. Chemical looping combustion of hard coal in a 1 MWth pilot plant using ilmenite as oxygen carrier. Appl Energy 2015;157:288–94.

[107] Pikkarainen T, Hiltunen I, Teir S. Piloting of bio-CLC for BECCS. in 4th International Conference on Chemical Looping. 2016.

[108] Berdugo Vilches T, et al. Experience of more than 1000h of operation with oxygen carriers and solid biomass at large scale. Appl Energy 2017;190:1174–83.

[109] Moldenhauer P, et al. The use of ilmenite as oxygen carrier with kerosene in a 300W CLC laboratory reactor with continuous circulation. Appl Energy 2014;113:1846–54.

[110] Moldenhauer P, et al. Chemical-looping combustion with fuel oil in a 10 kW pilot plant. Energy Fuel 2014;28(9):5978–87.

[111] Moldenhauer P, et al. Chemical-looping combustion with heavy liquid fuels in a 10 kW pilot plant. Fuel Process Technol 2017;156:124–37.

[112] Jerndal E, et al. Using low-cost iron-based materials as oxygen carriers for chemical looping combustion. Oil & Gas Science and Technology-Revue d'IFP Energies nouvelles 2011;66(2):235–48.

[113] Bidwe AR, et al. Use of ilmenite as an oxygen carrier in chemical looping combustion-batch and continuous dual fluidized bed investigation. Energy Procedia 2011;4:433–40.

[114] Kolbitsch P, et al. Operating experience with chemical looping combustion in a 120 kW dual circulating fluidized bed (DCFB) unit. Int J Greenhouse Gas Control 2010;4(2):180–5.

[115] Bao J, et al. Continuous test of ilmenite-based oxygen carriers for chemical looping combustion in a dual fluidized bed reactor system. Ind Eng Chem Res 2013;52(42):14817–27.

[116] Tang M, Xu L, Fan M. Progress in oxygen carrier development of methane-based chemical-looping reforming: a review. Appl Energy 2015;151:143–56.

[117] Luo S, et al. Shale gas-to-syngas chemical looping process for stable shale gas conversion to high purity syngas with a H 2: CO ratio of 2: 1. Energ Environ Sci 2014;7(12):4104–17.

[118] Kathe M, et al. Modularization strategy for syngas generation in chemical looping methane reforming systems with CO2 as feedstock. AIChE J 2017;63(8):3343–60.

[119] Kathe M, et al. Utilization of CO 2 as a partial substitute for methane feedstock in chemical looping methane–steam redox processes for syngas production. Energ Environ Sci 2017;10(6):1345–9.

[120] Hsieh T-L, et al. Chemical looping gasification for producing high purity, H2-Rich syngas in a cocurrent moving bed reducer with coal and methane cofeeds. Ind Eng Chem Res 2018;57(7):2461–75.

[121] Kong F, et al. Process intensification by applying chemical looping in natural gas to dimethyl ether conversion process—Implications for process design education. Chemical Engineering and Processing-Process Intensification 2019;143:107566.

[122] Karimi E, et al. Experimental study of chemical-looping reforming in a fixed-bed reactor: performance investigation of different oxygen carriers on Al2O3 and TiO2 support. Energy Fuel 2014;28(4):2811–20.

[123] Sun Z, et al. Chemical looping reforming of CH4 in the presence of CO2 using ilmenite ore and NiO-modified ilmenite ore oxygen carriers. Chem Eng J 2020; 401:123481.

[124] Lind F, et al. Ilmenite and nickel as catalysts for upgrading of raw gas derived from biomass gasification. Energy Fuel 2013;27(2):997–1007.

[125] Schmitt N, et al. Thermo-chemical conversion of biomass and upgrading to biofuel: The Thermo-Catalytic Reforming process – a review. Biofuels Bioprod Biorefin 2019;13(3):822–37.

[126] Ochoa A, et al. Coke formation and deactivation during catalytic reforming of biomass and waste pyrolysis products: a review. Renew Sustain Energy Rev 2020; 119:109600.

[127] Lind F, Seemann M, Thunman H. Continuous Catalytic Tar Reforming of Biomass Derived Raw Gas with Simultaneous Catalyst Regeneration. Ind Eng Chem Res 2011;50(20):11553–62.

[128] Mattisson T, Lyngfelt A, Applications of chemical-looping combustion with capture of CO2. Second Nordic Minisymposium on CO2 Capture and Storage, Göteborg, Sweden, 2001.

[129] Hedayati A, et al. Thermochemical conversion of biomass volatiles via chemical looping: comparison of ilmenite and steel converter waste materials as oxygen carriers. Fuel 2022;313:122638.

[130] Abad A, et al. Fuel reactor modelling in chemical-looping combustion of coal: 1. Model formulation. Chemical engineering science 2013;87:277–93.

[131] Pallarès D, Johnsson F. Macroscopic modelling of fluid dynamics in large-scale circulating fluidized beds. Prog Energy Combust Sci 2006;32(5–6):539–69.

[132] García-Labiano F, et al. Fuel reactor modelling in chemical-looping combustion of coal: 2—simulation and optimization. Chem Eng Sci 2013;87:173–82.

[133] Ohlemüller P, et al. Development and validation of a 1D process model with autothermal operation of a 1 MWth chemical looping pilot plant. Int J Greenhouse Gas Control 2018;73:29–41.

[134] Gayán P, et al. Assessment of technological solutions for improving chemical looping combustion of solid fuels with CO2 capture. Chem Eng J 2013;233:56–69.

[135] Abad A, et al. Conceptual design of a 100 MWth CLC unit for solid fuel combustion. Appl Energy 2015;157:462–74.

[136] Lyngfelt A, Leckner B. A 1000 MWth boiler for chemical-looping combustion of solid fuels–discussion of design and costs. Appl Energy 2015;157:475–87.

[137] Sandu V-C, Cormos A-M, Cormos C-C. Fuel reactor CFD multiscale modelling in syngas-based chemical looping combustion with ilmenite. Energies 2021;14(19): 6059.

[138] Gallucci F, et al. Experimental demonstration of chemical-looping combustion of syngas in packed bed reactors with ilmenite. Chem Eng J 2015;274:156–68.

[139] Symonds RT, et al. Systems analysis of pressurized chemical looping combustion for SAGD applications. Int J Greenhouse Gas Control 2018;73:111–23.

[140] Cabello A, et al. Economic analysis of pressurized chemical looping combustion for steam assisted gravity drainage applications. Int J Greenhouse Gas Control 2019;90:102786.

[141] Stevens RW, et al., Oxygen carrier production cost. 2019, National Energy Technology Laboratory (NETL), Pittsburgh, PA, Morgantown, WV ….

[142] Zhu L, et al. Tech-economic assessment of second-generation CCS: Chemical looping combustion. Energy 2018;144:915–27.

[143] Tsupari E, Tähtinen M, Kärki J. Feasibility of solid fuel CLC plant investment in the future energy systems including high share of solar and wind. Energy Procedia 2014;63:7508–16.